2008

REPRESENTATIONS OF HORIZONTAL HEAD-ON-BODY POSITION IN THE PRIMATE SUPERIOR COLLICULUS

Benjamin Nagy
Western University

REPRESENTATIONS OF HORIZONTAL HEAD-ON-BODY POSITION IN THE PRIMATE SUPERIOR COLLICULUS

(Spine title: REPRESENTATIONS OF HEAD POSITION IN THE SUPERIOR COLLICULUS)

(Thesis format: Monograph)

by

Benjamin Nagy

Graduate Program in Neuroscience

A thesis submitted in partial fulfillment
of the requirements for the degree of
Master of Science

Faculty of Graduate Studies
The University of Western Ontario
London, Ontario, Canada

Certificate of Examination

Supervisor	Examiners
Dr. Brian Corneil	Dr. Stephen Lomber
Supervisory Committee	Dr. Blaine Chronik
Dr. Stefan Everling	Dr. Tutis Vilis
Dr. Paul Gribble	

The thesis by

Benjamin Nagy

Entitled:

Representations of horizontal head-on-body position in the primate superior colliculus

is accepted in partial fulfilment of the
requirements for the degree of
Master of Science

Date_____

_____
Chair of the Thesis Examination Board

Abstract

To further elucidate the role of the superior colliculus (SC) in the control of gaze, I recorded from neurons within the primate SC while altering head-on-body position. I rotated the torso under a head fixed in space to determine whether proprioceptive information from neck muscles affected gaze-related neural activity. 50 of 60 movement-related neurons showed movement-related activity that was linearly modulated as a function of head-on-body position, with an average change in discharge rate of 0.89 spikes per second per degree of body rotation. Many neurons with visual and delay activity also exhibited head-on-body position-dependant modulation. The results of this study suggest that the SC has access to proprioceptive information, and that this information may be transmitted to downstream brain centres that execute gaze shifts.

Key Words

superior colliculus; gaze shift; gain field; motor control; proprioception; neck muscle; head position

Co-Authorship

I, Benjamin Nagy, am submitting this research project as partial fulfillment of the Master of Science Degree in the discipline of Neuroscience. As such, I have assumed a primary role in all aspects of this document including, but not limited to, laboratory setup, experimental design, data collection and analysis, as well as producing the initial draft of the thesis. Dr. Brian D. Corneil acted as my supervisor for this project. He provided the framework for this project as well as providing critical advice throughout all stages, and also acted as an editor to the subsequent drafts of this thesis. Tania Admans provided the initial training of the animals used in this thesis.

Acknowledgements

I would like to first thank my supervisor, Dr. Brian Corneil, for his support and guidance these past few years. Not only has he helped me with the development of this thesis, but he has taught me what it means to be a scientist and researcher. He has always been there whenever needed, and his dedication to me and this project has been tremendous.

I would also like to thank Dr. Stefan Everling, who has kept me company at the Centre for Brain and Mind during my stay. His advocacy and fervent support for scientific research has been a constant source of motivation.

Thanks also goes to Dr. Paul Gribble, who has spent equal time teaching me the principles of statistical analysis, and helping me find out what I should do with my life. I have made progress in both, though more in one than the other.

All of my friends at Robarts, both staff and students, also deserve many thanks. They have kept the facility running, making this research possible, and they have kept me running as well – I can't imagine how I would have survived so far away from home without their friendship.

Table of Contents

List of Figures

List of Appendices

List of Abbreviations

ANOVA	Analysis of Variance
EMG	Electromyographic
EPSP	Excitatory Postsynaptic Potential
FEF	Frontal Eye Fields
LED	Light Emitting Diode
LIP	Lateral Intraparietal Area
LTA	Linear Trend Analysis
MRI	Magnetic Resonance Imaging
PPC	Posterior Parietal Cortex
SC	Superior Colliculus

List of Symbols

°	Degrees
±	Plus or Minus
Ω	Ohms
A	Amperes
cd	Candela
ft	Feet
Hz	Hertz
g	Grams
mm	Millimetres
ms	Milliseconds
s	Seconds

Chapter 1 - Introduction

1.1 Sensory-Motor Transformations and Frames of Reference

For an organism to be successful, it must act in ways that bring benefit and avoid harm. Ultimately, all things good and bad come from one's environment, and in order to survive, information must be perceived and interpreted so that appropriate action can be taken.

Imagine a single-cell with sensory receptors and locomotor organelles located throughout its surface. This cell may do quite well by detecting bio-chemical gradients in its environment and initiating movement either towards or away from the perceived source. A threat, for example, from one side of the cell may activate flagellum on that same side, rapidly moving the cell to safety. In such a case, converting sensory information into a motor command involves no directional transformation.

More complex organisms, however, tend to have sensory and locomotor organs that are directional in nature. The tail on a fish has to be oriented against the direction of desired motion to be effective, just as most mammals can run forward much more effectively than they can run sideways or backwards. Similarly, many animals have directional sensory organs, such as eyes, that cannot perceive all of the surrounding space simultaneously, and require repeated repositioning for the complete examination of the environment. Many animals have also evolved a mobile head – that is, a head that is mobile on the body – and this allows an animal to run or fly in one direction, while receiving sensory information from a different direction.

Let us say that I am searching for my missing coffee cup. I walk around, scanning all the possible locations in which I may have left it. Finally, I catch a glimpse of the mug out of the corner of my eye, and I turn my head to one side and focus my gaze straight at it – I have found it! Now, what do I do? Can I reach straight ahead and grab the mug? Even though I am looking directly at the mug, this does not imply that I can simply extend my arm forward to grasp it. My gaze is off to the side, and "straight ahead" has a different meaning depending on whether I am considering my eye's, body's, or arm's perspective. I may reach forward, only to unintentionally knock over something that was straight ahead of *my body*.

Clearly, sensory and motor organs and limbs are often not aligned, and in order to effectively interact with the perceived world, their respective locations have to be known. In the case of higher primates, including humans, such concerns are very important because of our propensity to use our hands to interact with many objects. My motor system has to know where my eyes are in my head, and where my head is on my body, so that when I attempt to pick up an object that I am looking at, I instinctively know whether I should move my hand straight ahead, to the right, or the left.

Finding the neural correlates to such tasks has been an area of major study over the last few decades. Some of the major questions that have been asked include: how does the brain code the location of stimuli, and how does the brain keep track of the position of sensory and motor organs and limbs?

Two common ways in which we consciously identify the location of an object in space is through world-centred and body-centred frames of reference. Consider the coffee cup, resting on a table. As I walk around the table, the cup does not move, and my perception of the cup is one of stability in the world. The cup is on the table, which is on the floor, which is attached to the earth. A world-centred frame of reference is sometimes also known as earth-centric. At the same time, as I walk around the cup, I also perceive my own motion, and I perceive that my position relative to the cup is changing. The cup may be in front of me, behind me, or to either side; its distance away from me may also vary. Defining the location of an object relative to my own location would be using a body-centred, or ego-centric, frame of reference.

While I am looking at this cup, I can reach out, grasp the handle, and pick up the cup with relative ease. I can do this while I stand facing the cup, but I can also do this with my side towards the cup, or while sitting in a chair next to the cup. These reaching and grasping manoeuvres are very different from one another, yet I know exactly how and where to move my hands in order to grasp the cup, no matter my position relative to it. In order for me to do this successfully, I must be aware of the location of the cup relative to my body, and to the existing location of my arm and hand. Unless I have already made direct physical contact with the cup (which would most likely occur based on prior visual information) my hand possesses no remote sensors that could tell me where, with respect to my hand, the cup is located. All I have to go on is what I can see with my eyes.

My eyes see the cup, by definition, in retinal coordinates. The location of the cup's image on my retina provides information about where the cup is relative to where my eyes are directed. If I am looking directly at the cup, then the cup is "straight ahead" of my eyes. If for this example, we consider that my eyes are rotated in their orbits by 20° towards the right, then the cup would be 20° to the right of my head. Knowing the position of my head on my torso I can now localize the cup with respect to my body. For example, if my head is 30° to the left of my torso, then 20° rightwards - 30° leftwards = 10° leftwards (see Figure 1, subfigure A). Now, if I wanted to pick up this cup, I know it is 10° to the left of my body. Of course, this is only half of what is necessary – I also need to move the joints in my shoulder, elbow, wrist, and fingers – requiring a combination of angles that ultimately sum so that my hand arrives at the desired location to grasp the cup. As with the eyes and head, the cup's location can be considered from the perspective of each individual muscle – do they need to contract or relax, and if so, how much – in order to get my hand closer to the cup. In this sense, the cup also has representations in individual muscle-centric frames of reference.

1.2 Gaze Shifts as a Model for Motor Action

The number of coordinate transformations involved in visually locating and then grasping a cup are quite numerous, and span many frames of reference. A simplified model, used frequently in studies of reference frames and coordinate

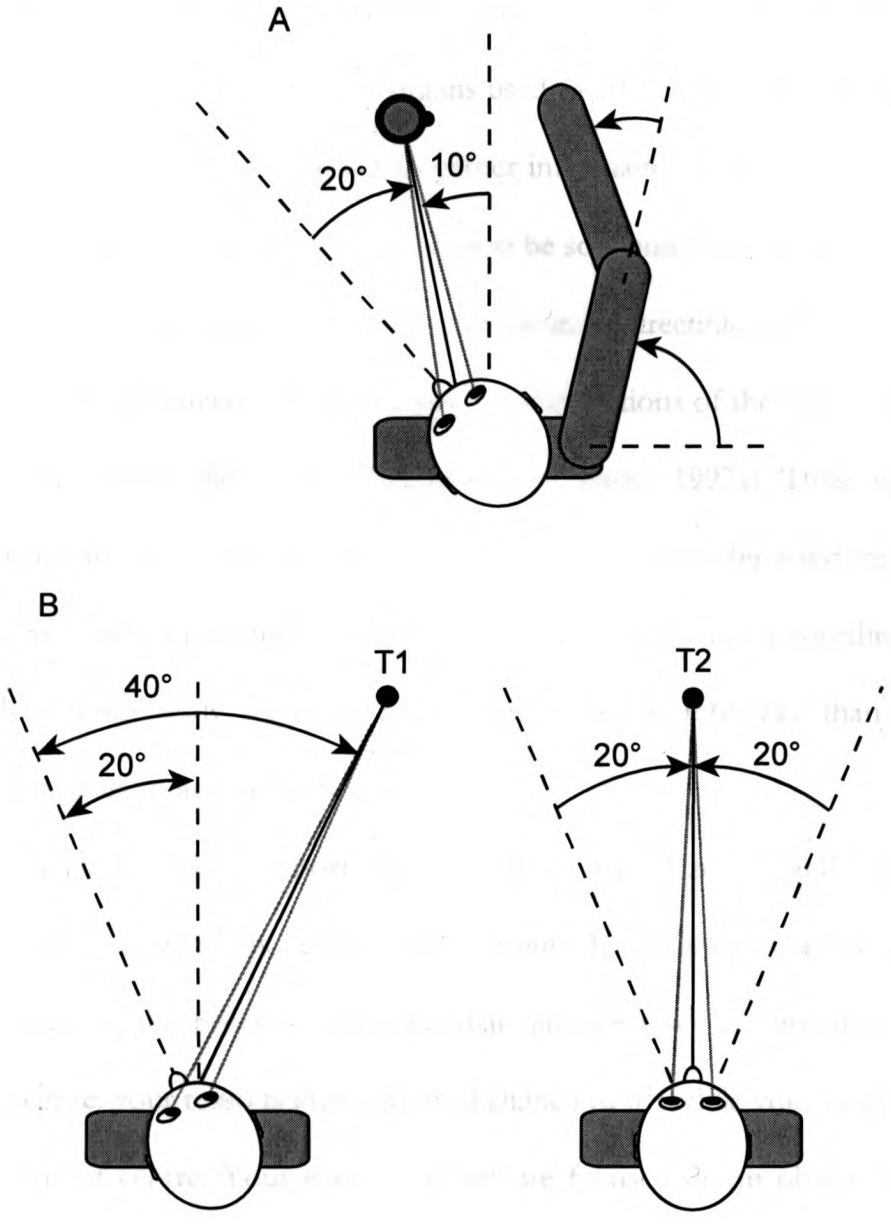

Figure 1. Reference Frames. A: The location of an object in eye, head, and body centred coordinates. Eye-in-head position must be combined with head-on-body position to locate the object relative to the body. Reaching out to grasp the object also requires a combination of angles between at the shoulder and the arm. Thus, the entire system has transformations at the level of the eye, head, body, shoulder, elbow, and in practice, also the wrist and fingers; an object can be localized relative to any of these body parts. B: Illustrations of the initial and final eye, head, and body positions for an example gaze shift that starts 20° to the right of the body (T1) and ends at 0° relative to the body (T2). The initial and final target position is to the right of the head, but the final target position is to the left of the eyes. The gaze shift results in a 20° rightward head-on-body movement, and a 40° leftward eye-in-head movement, resulting in a 20° leftward gaze (eye-in-space) movement.

transformations, is one that looks purely at the gaze aspect of the above example. We often think of our limbs as motor organs used to affect the world around us, and of our eyes as sensory organs helping us gather information from our surroundings. But as we know, the eyes are mobile – and must be so – and thus the act of collecting visual information is not a purely passive endeavour. Redirecting one's eyes is termed a *gaze shift*, and these movements sometimes involve motions of the head and torso as well (McCluskey and Cullen, 2007; Freedman and Sparks, 1997a). These gaze shifts are similar in many ways to typical limb movements, but can offer a reduced level of complexity for study. The transformation of a visual stimulus into a coordinated gaze shift involves fewer body segments and fewer frames of reference than a similar transformation into an arm or limb movement.

To illustrate the importance of reference frames and coordinate transformations to gaze shifts, let us refer to Figure 1, subfigure B, and consider an example similar to the previous, but one that highlights several important aspects particular to gaze: your torso is immobile and aligned to 0°, while your head is turned 20° to the left of centre. Your eyes, however, are focused on an object 20° to the right of centre (T1), and thus your eye-in-head position is 40° to the right. You want to make a gaze shift to a new location straight ahead of your torso (T2). Let us say, in this example, that the gaze shift involves both your eyes and your head moving towards the target. Your eyes will move left, and your head will move to the right. If both of these components align with the final target after the gaze shift, then your head will have moved 20° right to centre, and your eyes will have moved 40° left, in

their orbits, to centre. These two components sum to make the desired 20° leftward gaze shift.

This example illustrates that the location of the new target in oculocentric coordinates (20° left of the initial eye position) reflects neither the eye-in-head movement (40° left) nor the head-on-body movement (20° right). In order to move the head towards the goal, the goal location must be transformed from oculocentric coordinates into craniocentric coordinates. In this case, a leftward oculocentric goal must be transformed into a rightward craniocentric goal. Similarly, the oculocentric location of the goal also has to be transformed into a desired eye-in-head position so that the actual eye movement can be calculated with consideration for the head component of the movement.

Information regarding the locations of the eye in the head and the head on the body may come from several sources. One major candidate is proprioceptive output from the involved muscles. Information from muscle spindles provides information on the current position of a body segment (Matthews, 1982; Gandevia et al., 1992). Neck muscles have a very high concentration of these muscle spindles (Richmond and Abrahams, 1975; Bakker and Richmond, 1982), and are integral for a variety of sensory-guided actions that relay knowledge of head-on-body position (Andersen and Buneo, 2002). As shown in the previous illustrations, initial head-on-body position may determine whether the head has to move left or right to a particular target, and as such, neck muscle activation may vary for different initial head-on-body positions (Corneil et al., 2001).

It is believed that the eye, with movements occurring very rapidly (up to 800°/s), does not provide proprioceptive information for tracking eye position in real-time, for the purposes of coordinating gaze shifts (Wang et al., 2007). Studies have shown that certain brain areas update eye position information *just before* the actual movement occurs, and that such an updating cannot be from proprioceptive signals, but is likely from what is known as efference copy or corollary discharge (Duhamel et al., 1992; Sommer and Wurtz, 2002). Instead of using sensory information to determine the position of a body segment, such as the eye, efference copy refers to a system of keeping track of motor outputs. This type of system works better for some situations over others. For example, the act of moving your arm may normally require a small amount of muscle recruitment, but it may also require a large amount of recruitment if you are lifting a heavy object or encounter dynamic resistive forces. Saccadic eye movements, which are rapid changes of eye-in-head position, are subject to a consistent amount of resistance, however, and making identical saccades from a (eye-in-head) location A to a location B can be accomplished using the same pattern of extraocular muscle recruitment (Robinson, 1964). Internally monitoring the activity of motor-related neurons allows for a consistent and fast source of real-time eye position information.

These two sources of eye-in-head and head-on-body positional information can provide the means necessary to allow targets to be transformed from oculocentric coordinates to craniocentric and body-centric coordinates for, among other things, the accurate execution of gaze shifts.

1.3 The Oculomotor System

The control of gaze is based up on a complex network that includes areas within the cerebral cortex, basal ganglia, thalamus, brainstem, and cerebellum (Leigh and Zee, 2006). Visual information is transmitted from the retina, through the lateral geniculate nucleus, to the visual cortex, where basic processing occurs. Two areas in the cortex that have neural activity correlated to gaze shifts are the frontal eye fields (FEF) and the lateral intraparietal area (LIP). While there are many similarities between these areas, the FEF have been shown to have activity related to intention, context, and goals (Everling and Munoz, 2000; Buschman and Miller, 2007). LIP, on the other hand, has shown activity related to multi-modal sensory integration, body configuration, and coordinate transformations (Andersen and Buneo, 2002; Andersen and Buneo, 2003; Buschman and Miller, 2007). Both FEF and LIP project to the superior colliculus (SC) in the brainstem (Stanton et al., 1988; Paré and Wurtz, 1997; Wurtz et al., 2001). Of these three brain areas, the SC is closest to the motor output and projects to eye and head premotor circuits further downstream in the brainstem (Isa and Sasaki, 2002; Sparks, 2002). It plays a crucial role in gaze shifts and is thought be a significant driver of movements. All three areas have been shown to activate prior to gaze shifts, and have neurons that code movements in oculocentric coordinates.

Neurons in these three areas all exhibit movement fields – that is, each neuron is active for a preferred movement vector. These neurons are broadly tuned, however, and also show some activation for gaze shifts of similar direction and

amplitude. These activation patterns, or movement fields, are typically considered Gaussian in shape, with the location of peak activity signifying the preferred vector.

A common effect that has been observed in all three areas has been the influence of initial-position. LIP has been shown to have neural activity modified by initial eye-in-head and head-on-body position (Snyder et al., 1998; Andersen et al., 1990), and both FEF and SC have been shown to have activity modified by eye position (Van Opstal et al., 1995; Campos et al., 2006; Cassanello and Ferrera, 2007a). This influence of initial position manifests as a *gain field*, or a gain modulation of gaze-related activity as a function of initial position. This can be seen as a linear scaling of activity, with the curve maintaining its general shape and tuning. Figure 2 illustrates the shape of a typical movement field, and the effects that a modulating input may have.

Gain fields have been most thoroughly studied in the posterior parietal cortex (PPC), which includes LIP, and have been shown to be modulated by initial eye, head, or limb position. Current theories of the PPC highlight its role in multi-modal sensory integration and coordinate transformations between reference frames, and it is believed that these gain fields play a key role in these processes (Andersen and Buneo, 2002; Andersen and Buneo, 2003).

Theoretical studies have shown that gain fields can be used as a computational mechanism by which information can be transformed between coordinate frames

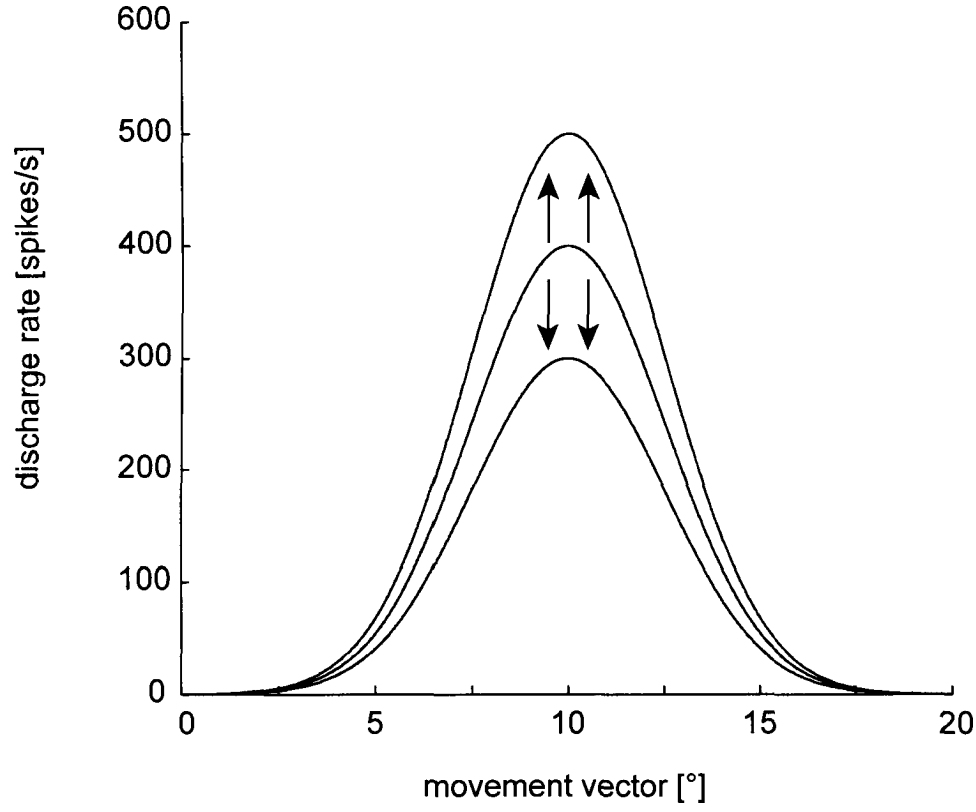

Figure 2. A typical gain modulated movement field. Target eccentricity is measured along the x-axis, while neural discharge rate is measured along the y-axis. Scaling does not affect the centre of the movement field, which is stable at 10°, but multiplies the discharge rate in a linear fashion. Such modulation of the movement field is also known as a gain field.

(Andersen and Buneo, 2002; Andersen and Buneo, 2003). Populations of cells that have oculocentric response fields that are modulated by various body position signals can be read out in multiple frames of reference (Pouget and Snyder, 2000; Xing and Andersen, 2000; Van Opstal and Hepp, 1995), suggesting space may be represented in a complex fashion, with cells potentially representing multiple reference frames simultaneously. In addition to coordinate transformations between reference frames, gain fields may also have roles in attention, navigation, decision making, and even object recognition, although some of these function lie outside the realm of the oculomotor system (Salinas and Thier, 2000).

While roles for gain fields in LIP and the PPC are generally believed to process coordinate transformations, gain fields in FEF and the SC are less well understood. It has been suggested that gain fields in FEF may be associated with remapping or target memory during gaze shifts (Cassanello and Ferrera, 2007a; Cassanello and Ferrera, 2007b). In the SC, gain fields have been hypothesised to represent a type of multi-code output where both desired gaze displacement and information about initial position can be transmitted further downstream. Information may be extracted from this combined output to be used in assisting the decomposition of a gaze shift into appropriate eye and head component movements (Van Opstal et al., 1995; Campos et al., 2006).

1.4 The Superior Colliculus

The SC, located in the midbrain, is a multilayered structure that receives inputs not only from cortical but also subcortical oculomotor areas (Sparks and Hartwich-Young, 1989). While the superficial layers of the SC receive projections from both the visual cortex and directly from the retina (Tigges and Tigges, 1981), the intermediate and deeper layers of the superior colliculus receive projections from LIP (Blatt et al., 1990; Paré and Wurtz, 1997) and FEF (Stanton et al., 1988; Segraves and Goldberg, 1987; Sommer and Wurtz, 2000), and project axons to various reticular nuclei involved in both eye and head motion (Moschovakis et al., 1996; Scudder et al., 1996a; Scudder et al., 1996b; Isa and Sasaki, 2002).

The SC has been shown to contain movement-related neurons whose discharge patterns are associated with eye-head gaze shifts, with particular neurons discharging for gaze shifts of particular vectors (Freedman and Sparks, 1997b). Freedman and Sparks examined single-unit neural activity in the SC and its correlation with the individual eye and head movements, and with the combined eye-head gaze movement. They showed that the burst of activity was most strongly correlated with the combined eye-head gaze vector.

Stimulation of specific sites within the SC has been shown to elicit contralateral eye-head gaze shifts with specific gaze vectors (Freedman et al., 1996). With stimulation parameters and location kept constant, gaze shifts of constant direction and magnitude are generated. Eye and head components of stimulation-driven gaze shifts can vary, but the combined eye-head gaze vector remains the same.

These studies suggest that high-frequency bursts of action potentials from the SC provide a gaze displacement command and that neurons in the SC have movement fields that are tuned to the target location in oculocentric coordinates. These studies are not in conflict with the gain field studies in the SC, which also showed that tuning remains oculocentric and stable. Though SC activity may be most strongly correlated with eye-head gaze displacement, this does not exclude gain field encoding with modulations that leaves neural tuning intact.

While the SC receives saccade-related inputs from LIP and FEF, additional inputs to the SC include projections shown in monkeys from neck muscle afferents to brainstem areas critical to the control of gaze, and which in turn project to the SC (Edney and Porter, 1986). Similarly, stimulation studies in anesthetised cats have shown that excitation of neck muscle afferents activate cells throughout the superficial and deeper layers of the SC (Abrahams and Rose, 1975). These studies suggest that not only does the SC receive saccade-related inputs from cortical areas, but may also receive information related to head position.

1.5 Purpose and Hypothesis

The presence of eye position gain fields in LIP, FEF, and the SC illustrates that initial eye position is incorporated in both the early and the later levels of the oculomotor system. Findings of head position gain fields in LIP may serve roles similar to that of the eye position gain fields, and as such, they may also be found in the FEF and SC.

I hypothesised that the SC participates in the transformation of the gaze displacement command from an oculocentric reference frame into not only a craniocentric but also a body-centric reference frame. Following this hypothesis would be the prediction that a gain field representation of head-on-body position may exist among the motor-related neurons within the primate superior colliculus.

The purpose of my study was to investigate the existence of head position gain fields in the SC, and to compare them to gain fields already found in the oculomotor system. This was done by performing extracellular recordings as head position was altered. Subjects' heads fixed in space while the torso was rotated – thus excluding vestibular inputs from the experiment and focusing exclusively on effects resulting from proprioceptive information. Neurons' movement fields were then analyzed and compared across body positions to determine the existence of linear gain modulation.

Chapter 2 - Methods

2.1 Animal Preparation

Two male rhesus monkeys (*Macaca mulatta*, monkeys *M* and *J*), weighing between 5.4 and 6.8 kg were used in these experiments. All training, surgical, and experimental procedures were approved by the Animal Use Subcommittee of the University of Western Ontario Council on Animal Care in compliance with the Canadian Council on Animal Care policy on the use of laboratory animals (see Appendix 1). Each animal's weight was monitored daily, and their general health was under the close supervision of the university veterinarians.

Each monkey underwent a surgical procedure to enable single-unit extracellular recordings from the superior colliculus, and to enable chronic eye position recording. To enable extracellular recording, a head implant of dental acrylic was anchored to the skull using titanium screws. The dental acrylic served as a base for the attachment of a recording cylinder (Crist Instruments) for access to the superior colliculus, and also the attachment of a titanium head post which would permit the restraining of the animal's head. The recording cylinder was positioned sterotaxically over a 19 mm diameter craniotomy centered over the midline. The cylinder was tilted approximately 38° posterior of the vertical axis to allow for surface-normal access to both the left and right colliculus (with stereotaxic coordinates of posterior 0.0, dorsal/ventral 15.0, right/left 0.0).

To enable eye position recording, prefabricated eye coils (3 turns of stainless steel, Teflon-coated wire, 19 or 20 mm in diameter) were implanted subconjunctivally

into both eyes (Judge et al., 1980) to allow the measurement of gaze shifts using the magnetic search coil technique (Fuchs and Robinson, 1966). Coil leads were passed subcutaneously to connectors embedded within the acrylic.

2.2 Experimental Techniques

For the duration of each experimental session, the animals were placed into a customized primate chair (Crist Instruments). The design of the chair allowed for the interlocking of the aforementioned head post, thus eliminating all head movement. The chair also permitted the computer-controlled rotation of the animal's torso, which was secured through the closing of a back plate and an interweaving bar that restrained the animal's chest and arms. This restraint restricted active movements of the animal's upper torso to less than 5°. The rotating chair allowed for the controlled rotation of the torso with respect to the head along the horizontal plane, with a maximum range of rotation of the body under the head spanning ±40°. The animals were monitored throughout the experimental session via infrared cameras positioned outside of their line of site, and through a torque sensor attached to the head post; this allowed for the monitoring of the animals' behaviour, torso position, and any attempts to actively resist the computer-controlled rotation. Additionally, subjects had previously implanted electromyographic (EMG) electrodes within their dorsal neck muscles (Elsley et al., 2007), providing a secondary measure of the subjects' responses to the rotation. The animals acclimatized very well to the experimental setup, and showed no signs of active resistance to torso rotation.

The experimental sessions were conducted in a dark and sound-attenuated room, and placed in a 3 × 3 × 3 ft^3 gaze-tracking coil system (CNC Engineering). The animals faced an array of over 500 red light-emitting diodes (LEDs) arranged such that they covered ±35° of the horizontal and vertical visual field. These LEDs provided the visual stimuli in the experimental paradigm detailed in the subsequent section. The LEDs were located along a flat horizontal-vertical rectilinear grid, 1.5 ft from the subjects' head. LEDs were spaced 2° apart from the centre of the grid to a horizontal and vertical eccentricity of 20°. Beyond 20°, the LEDs were spaced 5° apart.

The experiments were administered through an IBM-compatible computer, which served as the interface for controlling a National Instruments PXI experimental controller running custom LabView Real-Time programs. This system permitted centralised control over the LED grid, the position of the primate chair, and the monitoring of the subjects' gaze at a rate of 1 kHz.

2.3 Experimental Procedure and Behavioural Paradigm

The task of collecting neural data first required the localisation and characterisation of a saccade-related neuron in the intermediate and deeper layers of the superior colliculus. Several procedures were used to accurately locate the electrode within these layers of the superior colliculus. First, an initial MRI was performed to localize the superior colliculus relative to the recording chamber. Second, initial stimulation experiments were conducted to locate regions that drove

contralaterally-directed saccades at short latency (stimulation parameters: biphasic pulses of 0.3 ms duration, 300 Hz, 50 μA or less, 100 ms total stimulation length). Third, it was confirmed that the evoked saccades and isolated movement-related activity conformed to the known topographical map of the superior colliculus (Sparks et al., 1976; Robinson, 1972).

Tungsten microelectrodes (FHC, ME) of approximately 100mm in length and 0.22 mm in diameter were used to record neural activity in the SC, and ranged in impedance from 0.5 to 3.0 MΩ at 1kHz. The microelectrodes were used in conjunction with a hydraulic microdrive (Narishige MO-95) that allowed control of penetration depth over a range of 100 mm. Electrodes were lowered through 23-gauge guide tubes that were 20 to 23 mm in length. These guide tubes prevented deviations from the straight-line path of the electrodes, and provided an exit aperture that was approximately 2-3 mm above the superficial layers of the superior colliculus. The guide tubes were held in place by a Delrin grid (Crist Instruments) inside the recording chamber.

The animal was first required to generate saccades to LED targets presented pseudo-randomly, at a rate of approximately one saccade per 3 to 8 seconds. A saccade to the target was followed by a liquid reward. I monitored the electrical signal recorded by the microelectrode as I positioned it to sites within the superior colliculus where individual neurons exhibiting saccade-related activity could be isolated. Once such a neuron was isolated, I determined the range of saccadic directions and magnitudes for which the neuron was active (the neuron's movement

field), and which specific direction and magnitude elicited the greatest activity (the neuron's preferred vector) (Sparks et al., 1976). Once a sufficient amount of data was collected, I used a custom MATLAB program to measure the discharge of the neuron for each corresponding saccade, and provide the vector that elicited the greatest discharge.

The animals then performed the delayed saccade task as illustrated in Figure 3. This task introduces a temporal separation between the target presentation and the movement. The rationale behind this task is to allow the separation of the neural activity into three distinct phases: 1) transient visual activity in response to the presentation of the target; 2) delay activity during which the animal must hold central fixation; and 3) saccade-related activity corresponding to the motor command to perform the saccade. A neuron was considered to have significant visual activity if there was at least a doubling of spike density during the visual period when compared to spike density present prior to target presentation. Similarly, significant delay activity also required a doubling of spike density during the delay period when compared to the time prior to target presentation. Motor activity was considered significant when spike density was at least double the spike density present during the delay period.

The complete sequence of events for each trial was as follows. First, a diffuse background light (1.0 cd/m^2) was used to illuminate the experimental room for 500 to 1000 ms, in order to counteract dark adaptation. 300 ms following the removal of the background light, the central LED (the fixation point) was presented. The

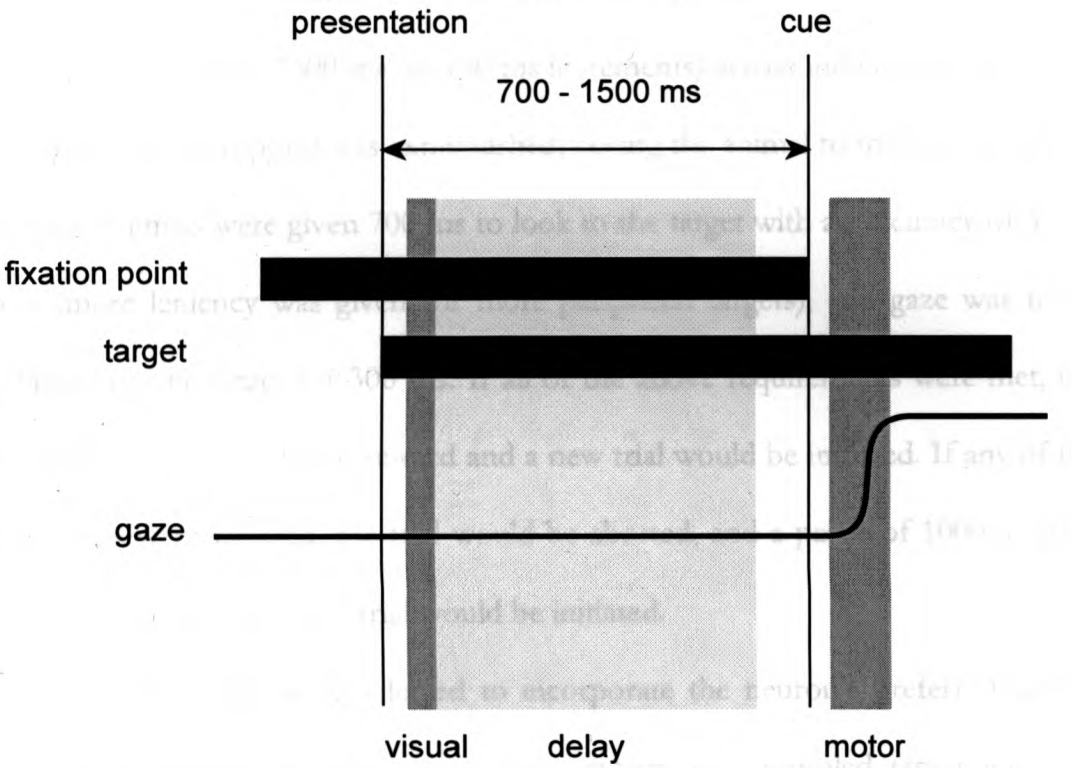

Figure 3. The delayed saccade paradigm. Subjects acquire the fixation point and maintain fixation. A target is presented ('presentation') while the fixation point is maintained for a variable period of time ranging between 700 to 1500 ms. The fixation point is deactivated ('cue') and signals to the subject to make a movement to the target location. The visual period ranges from 50 to 100 ms following target presentation, while the delay period begins immediately afterwards and extends to 100 ms prior movement onset. The length of the motor period was dynamic, and spanned 20 ms prior movement onset to 8 ms prior movement offset. The length of the motor period varied as a function of the movement duration.

animals were given 1500 ms to look to the fixation point within a 3° radius, and maintain central fixation for 750 ms. If fixation was maintained, a peripheral target LED was illuminated. With both the fixation point and the target illuminated, the animal was required to hold the fixation point for a pseudo-random period of time, varying between 700 to 1500 ms (in 100 ms increments) across individual trials. After this delay the fixation point was extinguished, cueing the animal to make a saccade to the target. Animals were given 700 ms to look to the target with an accuracy of 3 - 5° or less (more leniency was given for more peripheral targets), and gaze was to be maintained on the target for 300 ms. If all of the above requirements were met, the animals would receive a liquid reward and a new trial would be initiated. If any of the requirements were violated, the trial would be aborted, and a pause of 1000 to 2000 ms would ensue before a new trial would be initiated.

Target locations were selected to incorporate the neuron's preferred vector, and locations adjacent to this vector. Pilot experiments sampled target locations spanning both the horizontal and vertical extent of the movement field to permit examination of any changes in the movement field's characteristics. While I found no changes in the preferred vector over the course of this pilot experiment, I did find that this approach suffered from insufficient statistical power to determine the existence of a body-under-head position modulation effect. Thus, in subsequent experiments presented in this thesis, I limited the number of peripheral targets to those spanning a horizontal line through the preferred vector. An example set of targets is illustrated in Figure 4. This provided the statistical power to both observe

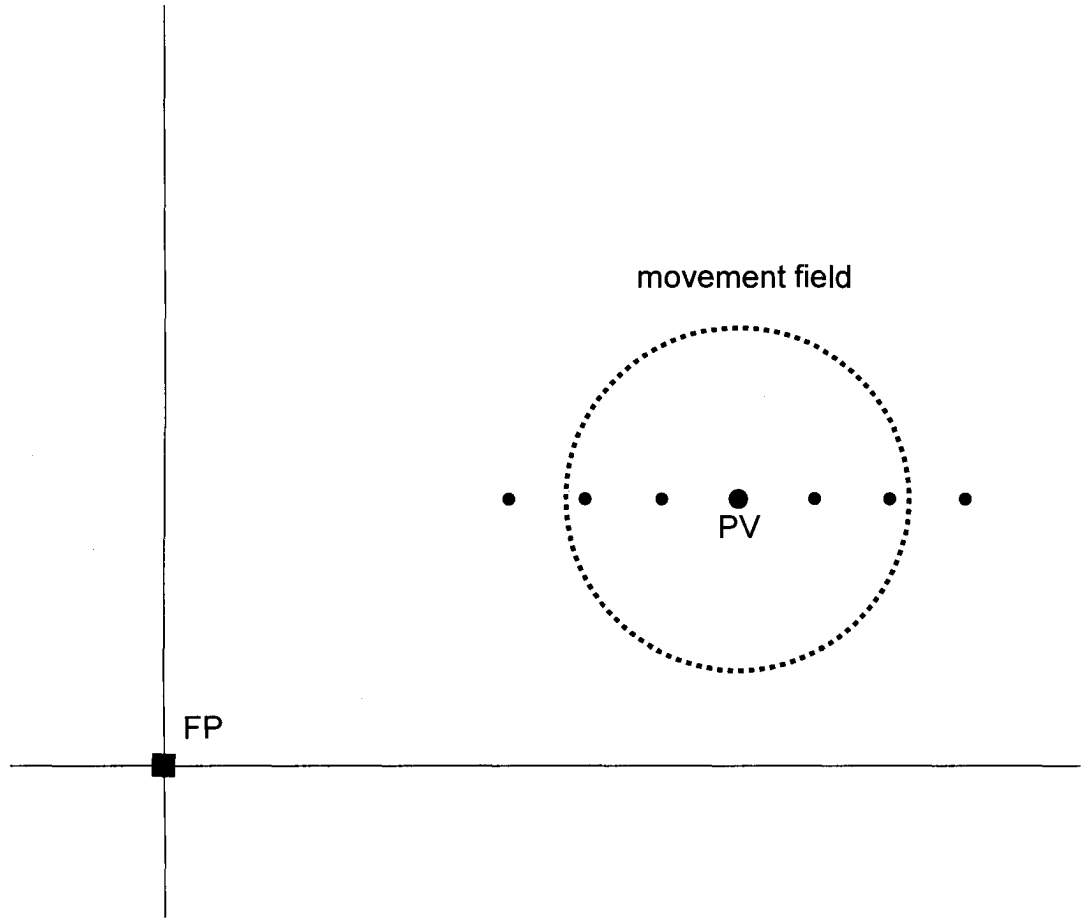

Figure 4. Example set of targets. FP denotes the fixation point (the origin in oculocentric coordinates), and PV denotes the preferred vector of a hypothetical SC neuron. The dashed circle encapsulates those vectors for which this neuron will activate and is also known as the movement field. There are 7 targets shown: a target at the preferred vector, and 3 targets to each side of the preferred vector. I attempted to quantify the movement fields of all recorded neurons using a horizontal set of targets that intersected the preferred vector and spanned the width of the movement field, as in this example.

any modulation, and to observe any changes in the neuron's movement field along the horizontal axis. Trials were performed repeatedly in blocks of 50 to 150 trials per block. Each block was carried out with the subject's torso in one of five pseudo-randomly selected body-under-head positions: -25°, -12.5°, 0°, +12.5°, and +25° (negative and positive values representing leftward and rightward positions, respectively). I defined a complete series of blocks as a minimum of 3 body-under-head blocks per series. The first 3 blocks that I collected were always at -25°, 0°, and +25°, in pseudo-random order. If the quality of the neural recordings permitted the ability to record further, I then ran blocks at -12.5° and +12.5°, also in pseudo-random order. Where conditions would allow, I repeated the 5 body-under-head blocks a second time. Thus, all series contained at least a minimum of 3 blocks with 150 total trials, up to 10 blocks with 1000 total trials. In most cases, I was able to obtain an average of 500 to 600 total trials.

2.4 Data Collection

Extracellular action potentials were sorted in real-time using amplitude and waveform criteria (Plexon Inc). The waveforms of valid action potentials were then saved at 40 kHz to file and then manually spike-sorted off-line using principal components, peak-valley, and spike energy analysis (Plexon Inc). Eye movements were first demodulated (CNC Engineering) and then sent to a customized LabView program for paradigm control. Eye movements were sampled at 1.0 kHz, recorded simultaneously with action potentials, and saved to the same file. Each trial was

manually examined off-line to confirm valid completion of the trial. The initiation and conclusion of a saccade was defined using a velocity criterion of 30 °/s. Any trials with anomalous eye movements, excessive delays, or multi-step saccades were discarded. Throughout the experiments, trials were rejected at a rate of less than 3%.

Each trial was then divided into three separate periods: visual, delay, and motor. The visual period was set to incorporate the peak of the visual burst, if present, and spanned from 50 to 100 ms following target onset (Sparks et al., 2000; Munoz and Wurtz, 1995). The size of the motor period was set to incorporate the peak of the motor burst, and spanned from 20 ms prior movement onset to 8 ms prior movement offset (Miyashita and Hikosaka, 1996; Campos et al., 2006; Van Opstal et al., 1995). These analysis windows were used for all cells, across all trials and body positions. The delay period spanned from 100 ms following target onset to 100 ms prior to movement onset.

Neural activity was quantified using two different methods: first, the number of spikes were counted within in each period, and then divided by the length of the period, resulting in an average measure of spikes per second over the duration of the period, or the average discharge rate. Second, a spike density function was generated by convolving the spike train with the excitatory postsynaptic potential (EPSP) function to represent the postsynaptic consequences of neural activity (Thompson et al., 1996):

$$y(t) = \left(1 - \exp\left(-\frac{t}{C_g}\right)\right)\left(\exp\left(-\frac{t}{C_d}\right)\right)$$

where t is time in milliseconds, C_g is the growth constant in milliseconds (1 ms), and C_d is the decay constant in milliseconds (20 ms).

Analysis of the visual and motor period used neuronal peak discharge rates extracted from the spike density function. The measurements of average discharge rate over these periods may have similar functional significance, and I found that my results showed no significant difference between analysis methods. This is not surprising since spike density based on the EPSP function defines the peak discharge rate based on activity over an approximately 50-100 ms window – which is comparable in length to the analysis windows used for the visual and motor periods for the calculation of average rates. To simplify the results for the visual and motor periods I will only present data generated from peak rates.

Unlike the short visual and motor periods, the delay period ranged in length from 700 to 1500 ms. As the spike density function can only capture activity within a 50 to 100 ms window, it would not be a suitable representation of delay period activity as a whole. Thus, in contrast to the other periods, results for delay period activity are calculated using the average rate method.

2.5 The Movement Field

The shape of movement fields for neurons in the SC are sometimes estimated as symmetric and Gaussian, however, more precise examination shows the movement fields of SC neurons as symmetric for vectors of constant magnitude with differing directions, but asymmetric for vectors of varying magnitudes with constant direction. As saccades are made that are smaller in magnitude than the centre of the movement field, a neuron's activity declines sharply, but as the saccade magnitude increases from the centre of the movement field, neural activity declines at a much slower rate (Sparks et al., 1976). For example, a motor-related SC neuron with a preferred vector of 10° to the left would have its peak discharge rate decline as saccades were angled up or down, but this decline would be symmetric. On the other hand, this same neuron may not discharge for saccades 5° to the left, but may show significant discharge rates for 15°, 20°, and 25° to the left. Refer to Figure 5 below.

Further studies have also suggested that neurons in the SC can be subdivided into two categories: those with open and those with closed movement fields (Munoz and Wurtz, 1995). A closed movement field is defined as having activity only for a narrow band of saccade vectors, while an open movement field has a similar rise in activity but is followed by an extended tail that remains stable as the saccade vector is moved further away. Mathematically, such an open movement field could be considered as an extremely asymmetric movement field with a very large width.

In order to accommodate movement fields with such spatially diverse discharge characteristics, I chose to quantify the movement fields by fitting a linearly

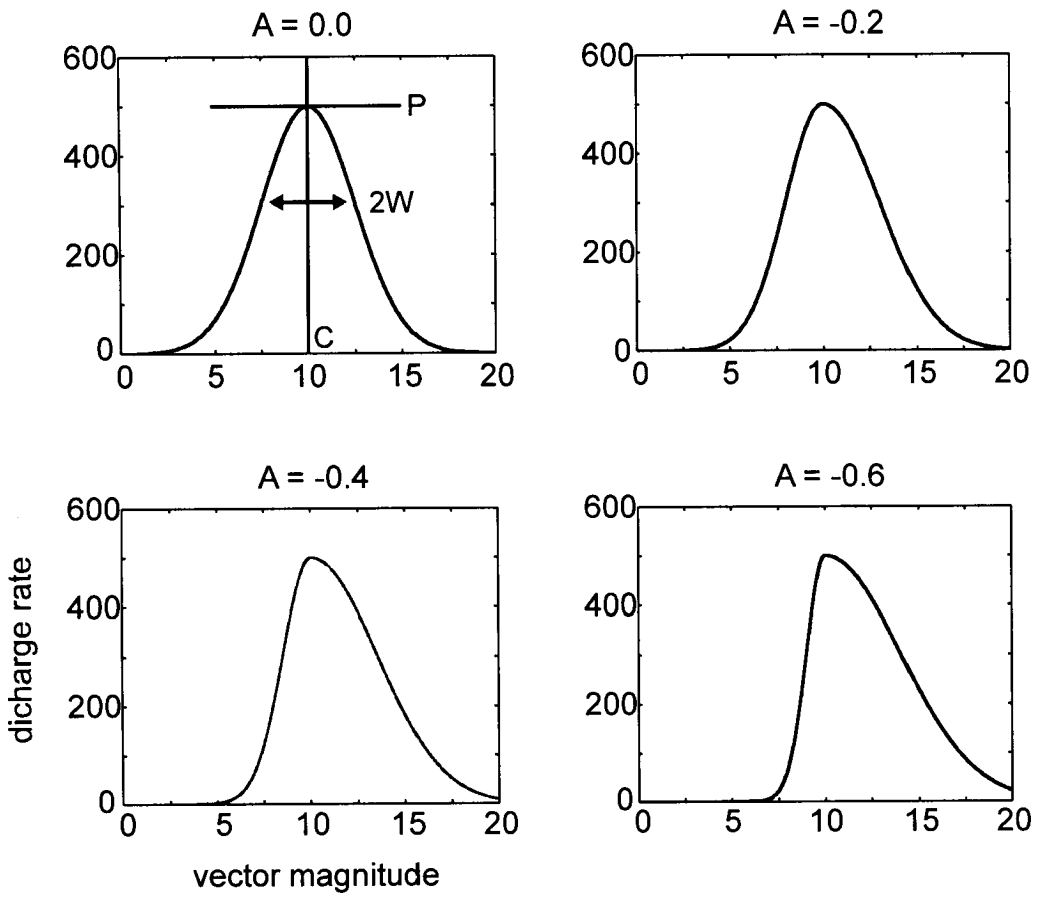

Figure 5. Gaussian asymmetry. These four subfigures show a Gaussian with constant *P*, *W* and *C* values. The symmetry parameter (A) is varied from 0.0 to -0.6. The width, centre, and peak of the curves remain the same, but the body of the curve tends towards right of centre.

asymmetric Gaussian to the data. This curve is similar to the following standard Gaussian curve:

$$y(x) = P\exp\left(-\frac{(x-C)^2}{2W^2}\right)$$

where x represents the horizontal component of the saccadic vector, P represents the amplitude of the Gaussian, C represents the centre of the curve, and W represents the width of the curve. W is typically defined as the standard deviation when a Gaussian is used to represent the normal distribution. In order to add a linear asymmetry, I add the A parameter, ranging in value between -1 and +1, as follows:

$$y(x) = P\exp\left(-\frac{(x-C+A|x-C|)^2}{2(W(1-A^2))^2}\right)$$

The A term in the numerator effectively scales the x-axis, while the A term in the denominator controls the width of the curve such that a constant W maintains the curve at constant width across all asymmetries. Figure 5 illustrates 4 curves with varying A as the other parameters are held constant.

Previous studies have used a log-Gaussian curve (Edelman and Goldberg, 2001; Bruce and Goldberg, 1985) to fit the movement fields of neurons in the SC and the FEF. This is a standard Gaussian curve that has been scaled logarithmically along its x-axis such that it can capture the asymmetric properties of a movement field. There were several reasons I chose not to use this curve for my fitting: first, this

curve does not fully capture the spatial properties of an open or partially-open movement field. Second, this curve's symmetry is determined by the location of its peak, and does not provide for independent scalability, nor the option to have no asymmetry at all. The log-Gaussian has been used to effectively represent movement fields along the radial direction only, however, my samples of saccadic movements cut a horizontal cross-section which may or may not line up with a field's optimal radial direction. Modifications to the log-Gaussian so that it could accurately represent a horizontal cross-section of a movement field increased computational requirements – and still failed to provide independent measurements of symmetry. A comparison of the fit errors between the asymmetric Gaussian and the log-Gaussian for several representative neurons (with *closed* movement fields) showed no statistical difference for preferred vectors along the horizontal-axis, but showed significantly poorer performance for preferred vectors with large vertical components.

Several of the neurons had movement field centres that were not completely captured due to experimental limitations: subjects were often reluctant to make saccades beyond 25°, thus any neuron with a field centre beyond this magnitude only had a portion of the movement field characterised. While my fitting curve was chosen because I found it to best approximate typical data sets, the quality of the fit deteriorated greatly if a large portion of the movement field was missing: if a neuron had a movement field center at approximately 35°, and I was able to capture its field from 0° to 30°, then it looked very much like a typical exponential function. In such a case, the Gaussian fitting procedure was unable to reliably find the movement field's

centre, and depending on where the centre was estimated to be, the peak discharge rate could vary by over 100%. This amount of variability prevented the calculation of any meaningful statistics, and so I settled on the following compromise: neurons with incomplete movement fields had their field centres estimated using the bootstrap fitting procedure, and then had their centres fixed to that value. While the meaning of such a fixed centre is questionable, it allowed for the measurement of changes in peak discharge rate without obscuring the results due to variability in the location of the field's centre. Because the entire movement field was not captured, I was unable to determine if the movement field centers were or were not moving, nor was I able to calculate a measurement of width. Thus, 5 neurons with incomplete movement fields were excluded from the analysis of movement field centres and widths.

I also recorded several neurons that appeared to have open movement fields. As mentioned before, these fields have a distinct rise in peak discharge rate, but have almost no decline as the saccadic magnitude is increased. The curve fitting bootstrap was able to accurately calculate the centre of the movement field as the location where discharge rates reached their initial maximum. The widths of these movement fields, however, were predictably calculated as approaching infinity. Since the width parameter has no meaning for neurons with open movement fields, 6 neurons with open movement fields were excluded from the analysis of movement field widths.

Measures of symmetry approached the maximum values of ± 1 for open movement fields. For neurons with incomplete fields, symmetry could not be calculated, and thus they were excluded from the symmetry analysis.

Chapter 3 - Results

3.1 Saccade-Related Activity

A total of 60 saccade-related neurons were recorded, 29 from monkey *M* and 31 from monkey *J*. All 60 neurons had a burst of activity in the motor period of the delayed saccade paradigm. 26 neurons also had a burst of activity in the visual period, and 28 had activity in the delay period. I recorded 28 cells with 3 body-under-head positions, 6 with 4 body-under-head positions, and 26 with 5 body-under head positions. Preferred vectors ranged in magnitude from 2° to 37°, with a mean of 13°; and ranged in direction from 63° downwards (from the horizontal axis) to 90° upwards, with a mean direction of 22° upwards. Using an example neuron, I will illustrate the quantification of the movement field, during the motor period, and the details of the analysis performed on all neurons. I will then show population results using the same analysis, for the entire set of neurons, for all periods.

Figure 6 shows neural activity for an example neuron as the subject made movements into the centre of the neuron's movement field. Rasters of action potentials and average spike density functions are shown for 3 body-under-head positions, with activity present for visual, delay, and motor periods. In this example, body-under-head position most visibly influenced the peak discharge rate during the motor period, with the greatest activity occurring when the body was 25° to the left.

A horizontal slice through the centre of this neuron's movement field is shown in Figure 7, for a body-under-head position of 0°. Peak discharge rates are

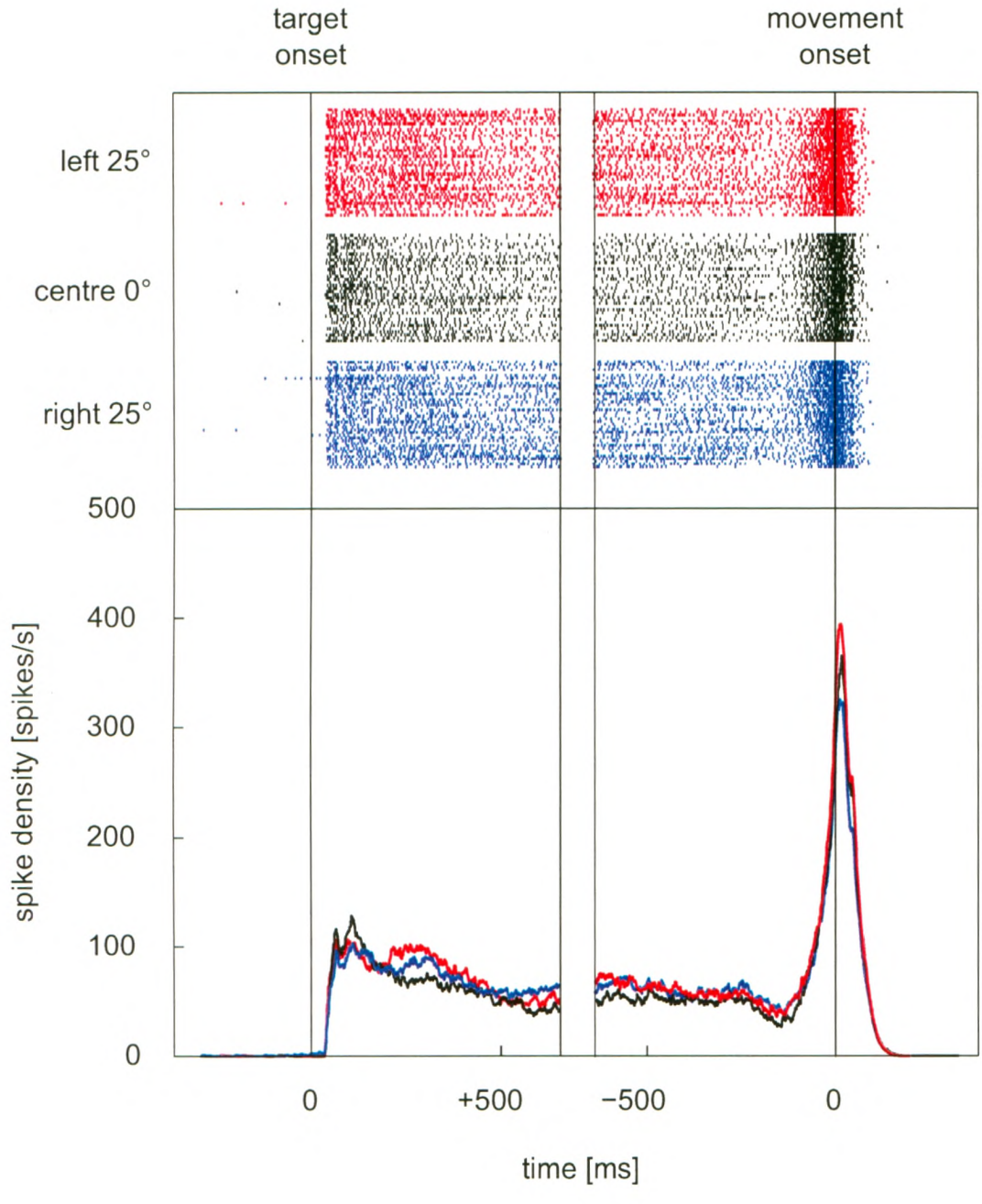

Figure 6. Spike rasters and spike densities for example neuron. Spike rasters (representing neural discharge) and average spike density functions (representing the rate of neural discharge) for 3 body-under-head positions are shown for the delayed saccade task, for gaze shifts to the centre of the movement field. Data is aligned to target onset on the left, and movement onset on the right. Each line of rasters represents neural discharge during a single trial. Average spike density functions were calculated by convolving each raster line with the EPSP function and averaging. As the body-under-head position is varied from left to right, the neural discharge rate during the motor period declines.

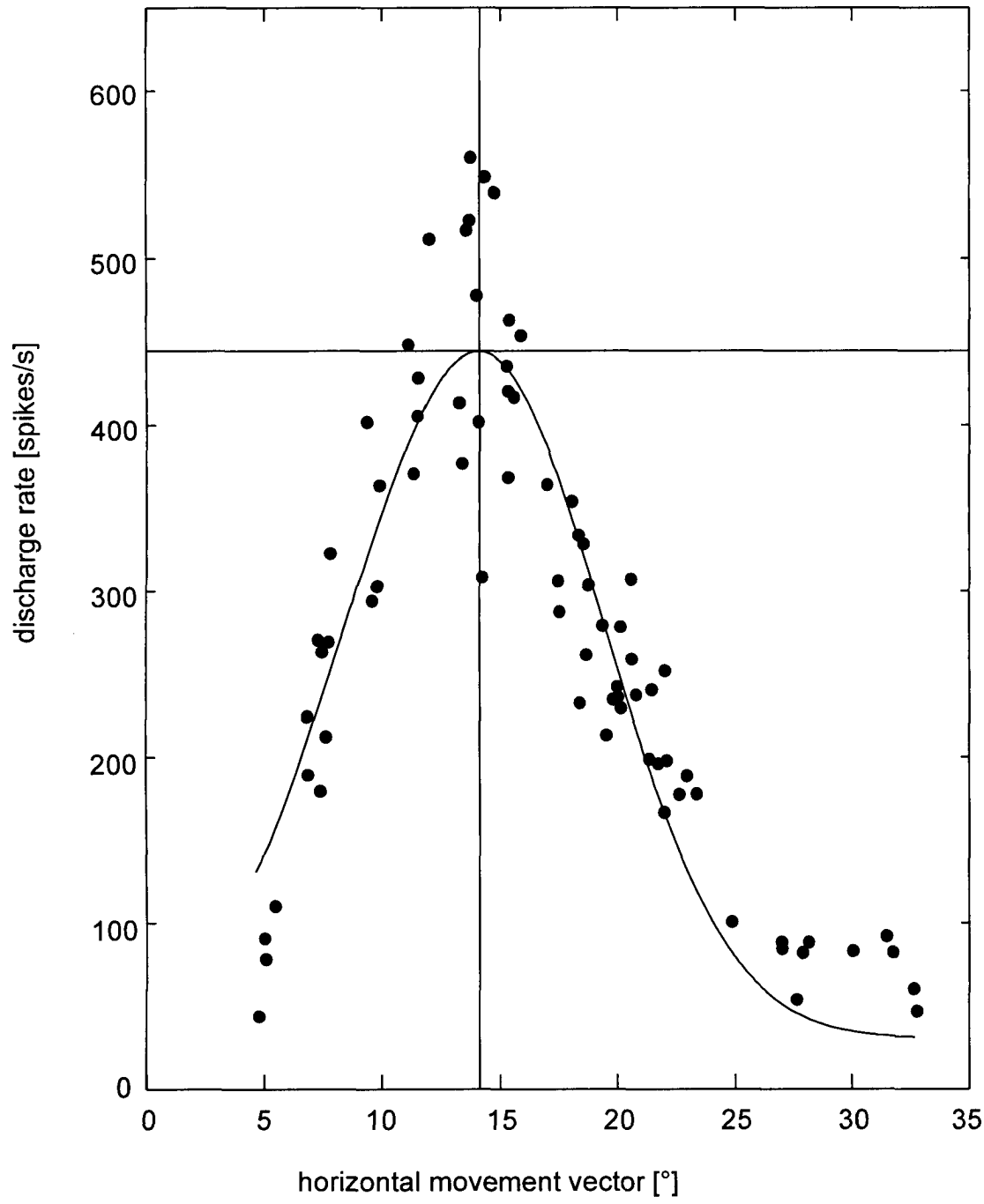

Figure 7. Movement field for example neuron, with a body-under-head position of 0°. Each point represents the peak spike density extracted from the motor period of a single trial, plotted as a function of the horizontal component of the saccade. A single linearly asymmetric Gaussian is fitted to the data, with a centre of approximately 14° rightwards, and a peak value of 444 spikes per second.

associated with movements of approximately 14° in the horizontal direction. Fitting an asymmetric Gaussian to the data quantifies the peak discharge rate, the centre, width, and symmetry of the field, as described above. What it does not provide, however, is any statistical information regarding the variability of these parameters. I therefore performed a bootstrap procedure to iteratively fit multiple curves to this data set. This entailed randomly selecting data points from the existing set, with replacement, to create a new data subset with the same number of data points. A curve was then fit to this new subset, and the parameters were extracted. This procedure was repeated 200 times, resulting in 200 estimates for the movement field's peak, centre, width, and symmetry. I then used these estimates to derive the variability present in the original data set. Such quantifying of variability permits statistical comparisons across various body-under-head positions.

3.2 Comparison of Movement Field Parameters Across Body Position

Blocks of data characterising a neuron's movement field, such as the one shown in Figure 7, were collected for each body position. Results for all 5 body-under-head positions are shown in Figure 8, for the motor period. As the body is rotated a total of 50°, the centre of the movement field, and its general shape, remain stable. The peak discharge rate at the centre, however, can be seen to decline as the body is rotated 25° left to 25° right. Values for peak discharge rate, as extracted from the bootstrap procedure, are shown in Figure 9. There appears to be a declining trend as the body-under-head position is rotated from left to right. Both an ANOVA and a

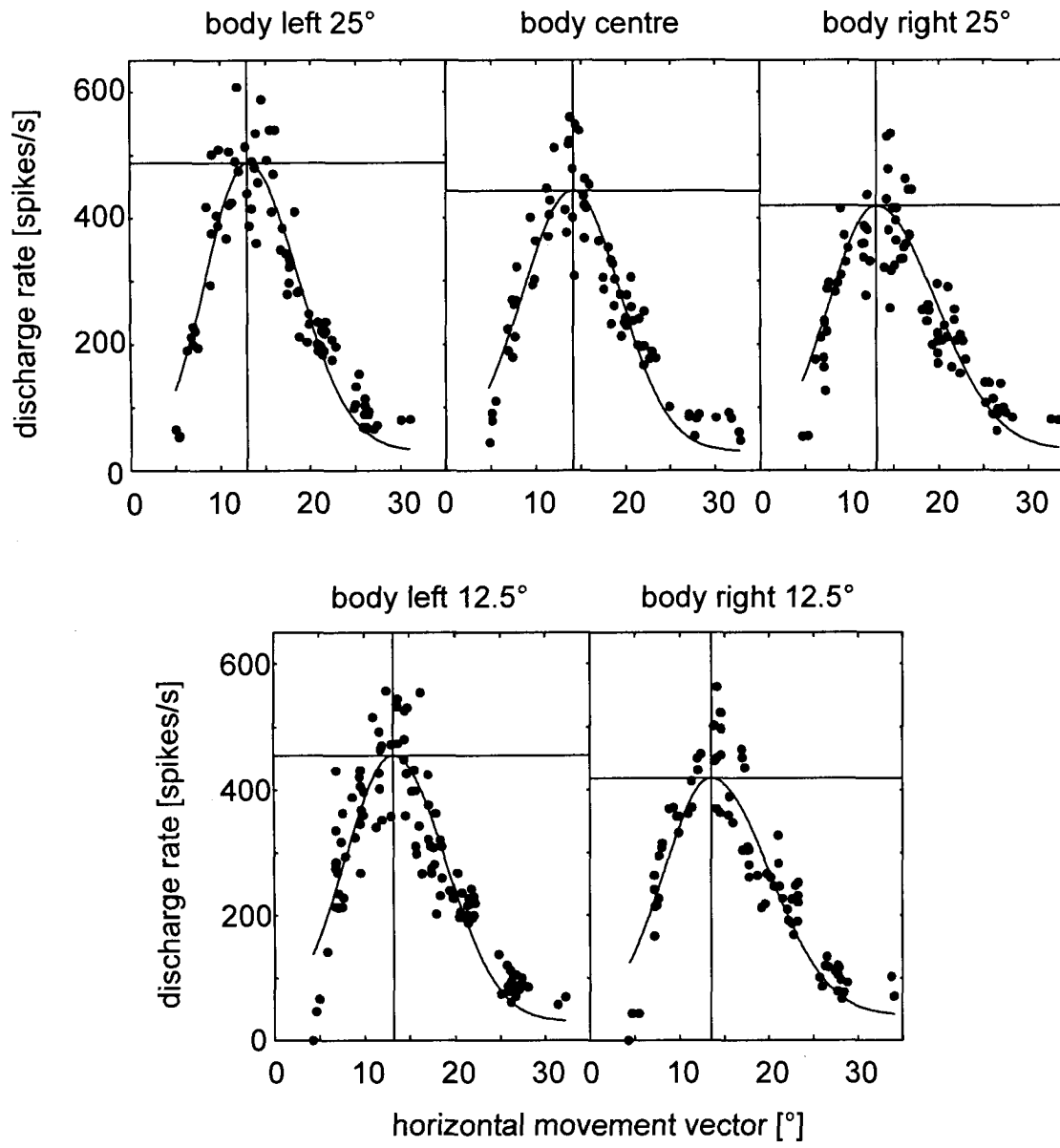

Figure 8. Movement field for example neuron, showing 5 body positions. Peak spike density during the motor period of the paradigm is shown, as a function of the horizontal component of the saccade. The shape of the Gaussian appears to remain the same as body position is rotated by a total of 50°, as does the location of the centre of the field. Peak discharge rates can be seen to decline, however, as the body-under-head position is rotated from 25° leftward to 25° rightward.

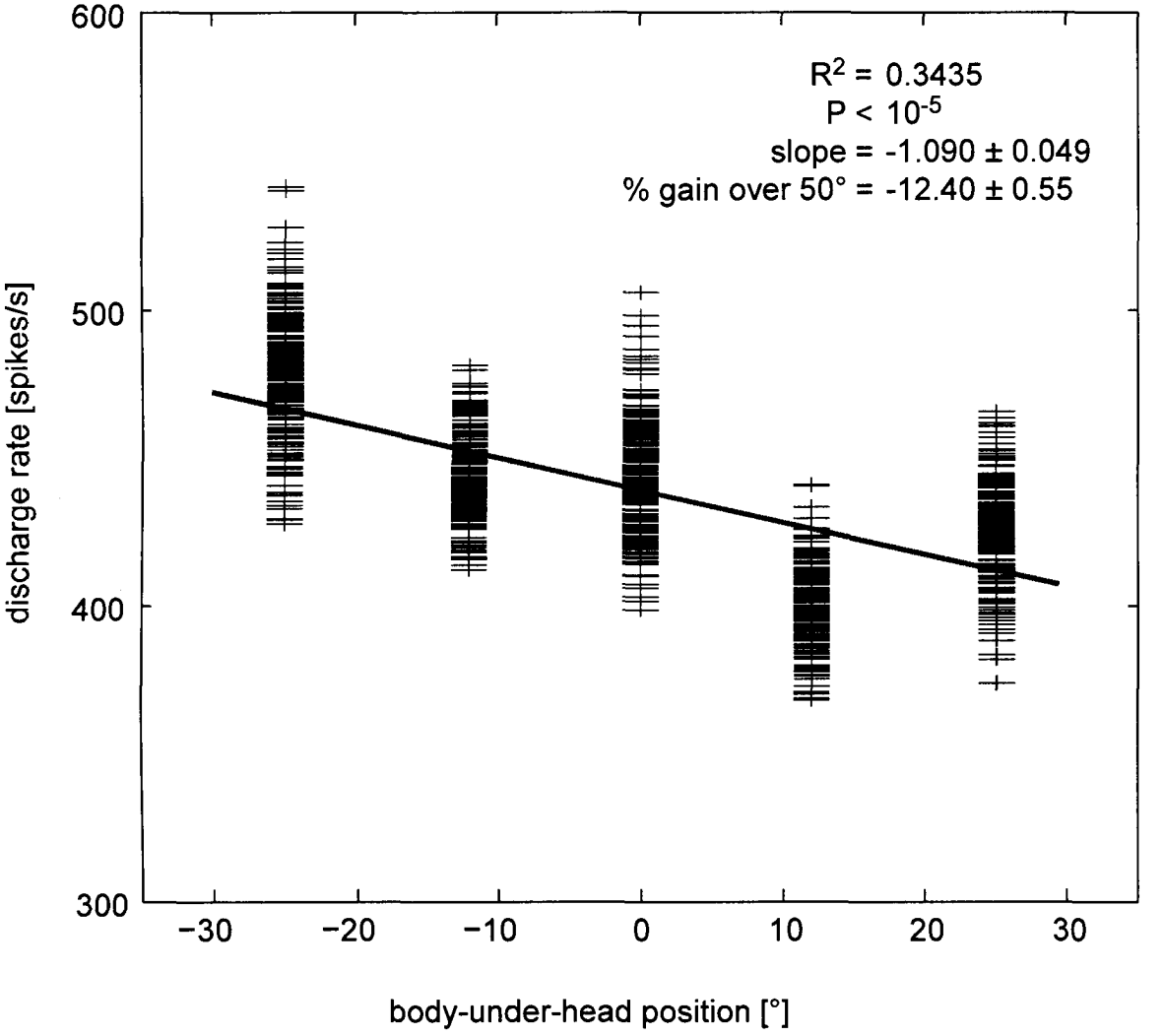

Figure 9. Bootstrap and linear regression results on example neuron. Peak discharge rates extracted from the bootstrap procedure are plotted as crosses, as a function of body-under-head position. A linear regression was employed to fit a trend line to the data, and is also shown. The decline in peak discharge rate has a significant linear component, with over 34% of the variance accounted for by the linear trend.

linear trend analysis (LTA) (Keppel and Wickens, 2004) show a statistically significant change in peak discharge rate as a function of body position (both $P < 10^{-5}$), with the latter confirming the linear decline.

To further examine and quantify the observed trend, a linear regression was performed to provide an estimate of the change in peak discharge as a function of body-under-head position, and to provide a measure of how much of the variability can be accounted for by such changes in position. The estimate provided by the linear regression is also shown in Figure 9, resulting in a trend of -1.10 ± 0.049 spikes/s per degree of body-under-head rotation (with $\pm$ values representing the standard deviation). This translates into a decrease in peak activity of about 55 spikes per second over 50° of body rotation, or a change of 12.4%. This analysis also shows that over 34% of the variability in peak discharge rate can be accounted for by this linear trend.

In the case of the movement field's centre, a change of only 0.009 ± 0.0014 degrees per degree of body-under-head rotation, or just under one-half degree across 50° of rotation, was detected. This is approximately two orders of magnitude smaller than the change in body-under-head position, and while statistically significant, shows that the movement field maintains its oculocentric tuning (and is not body-centric). An analysis of the width parameter results in a change of 0.016 ± 0.00041 degrees per degree of body-under-head rotation, which equates to 0.8° or 13% over 50° of rotation. Further discussion on the significance of the width parameter can be found in the Population Results section below.

The analysis of the unitless symmetry variable is slightly more complex than the others. Due to its arguably abstract representation of the shape of the movement field, its trend line is more difficult to interpret. In the case of the example neuron, no statistically significant linear trend was found ($P = 0.17$). The importance of this parameter should be noted, however, because significant changes in its value may signal a transition from a closed to an open movement field.

Detailed results for the example neuron are illustrated in Table 1 below. Only results from the motor period are presented here.

	Peak	Centre	Width	Symmetry
ANOVA	$P < 10^{-5}$	$P < 0.01$	$P < 0.01$	$P < 0.01$
LTA	$P < 10^{-5}$	$P < 0.01$	$P < 0.01$	$P = 0.094$
Linear Regression	$P < 10^{-5}$	$P < 0.01$	$P < 0.01$	$P = 0.17$
Trend Slope	-1.10 sp/s/°	0.0087°/°	0.0163°/°	—
Change Over 50°	-54.9sp/s	0.433°	0.817°	—
% Change Over 50° Relative To Value At 0°	12.4%	3.84%	13.4%	—
Regression r^2-Value	34.3%	3.28%	0.06%	—

Table 1. Statistical results for the example neuron, for the motor period.

The r^2-value from the linear regression assists in the interpretation of the results: a value of 34% means that one-third of the variations in the peak discharge rate of this cell can be accounted for by linear effects related to changes in body-under-head position. On the other hand, a value of 0.06% suggests that while a statistically detectable linear trend exists for changes in the width parameter, only

0.06% of the variations in the width can be accounted for by linear effects related to changes in body-under-head position.

While low r^2-values may be attributable to the inherent noise in the data, some additional considerations should also be made when considering the results of a linear regression. Firstly, if body-under-head position modulates the movement field in a non-linear fashion, the slope of the trend line merely represents a linear component of such a modulation. If the modulation is significant but non-linear, then the linear component of the fit may be very small. Similarly, the r^2-value of the regression will be small as well, since the linear component would only account for a small amount of the total modulation.

3.3 Population Results - Peak Discharge Rates

The analysis outlined above for the example neuron was performed on all neurons, and for all periods. Linear regression slopes were normalized for laterality such that they were defined as positive if they increased as the body was rotated towards the side of the movement field. For example, if a neuron's movement field was in the right visual field, then a positive slope would represent an increase as the body was rotated from 25° leftwards to 25° rightwards. Similarly, for the same movement field on the right side, a negative slope would result if a decrease was found as the body rotated from the left to the right.

An analysis of the peak discharge rates of the 60 neurons across body positions, during the motor period, yielded significant ANOVA results for 56 of the

neurons. Statistical significance in the following analysis is defined as a P-value less than 0.01. An LTA performed on these 56 neurons yielded significant results for 52. A linear regression was then run on these 52 neurons, and 50 yielded statistically significant non-zero results.

The average magnitude of the linear trends was found to be 0.893 spikes/s/°. Over 50° of body-under-head rotation, this equates to a change of 44.6 spikes/s. In terms of percentages, this amounts to a 0.476% change per degree of rotation, or 23.7% over the 50° of rotation. Of the 50 significant linear regressions, 33 neurons had an r^2-value over 10%. Likewise, 27, 20, and 14 neurons had r^2-values over 20%, 30%, and 40% respectively.

Figure 10 shows all significant linear trends for changes in peak discharge rate during the motor period. Subfigure A shows the distribution of slopes in terms of percentages, and illustrates the even distribution of positive and negative slopes. This means that as the body is rotated towards the side of the movement field, the peak discharge rate appears equally likely to rise as it is to fall. The average of all significant linear trends (positive and negative) is 0.136 spikes/s/°. This translates to 0.132 % per degree of body rotation, or 6.60% across 50° of body rotation. While a positive average slope may suggest a bias towards positive slopes overall, 25 of the 50 neurons show a positive trend, while 25 show a negative trend. A single sample t-test shows no significant difference from a mean of zero ($P = 0.22$), thus suggesting no

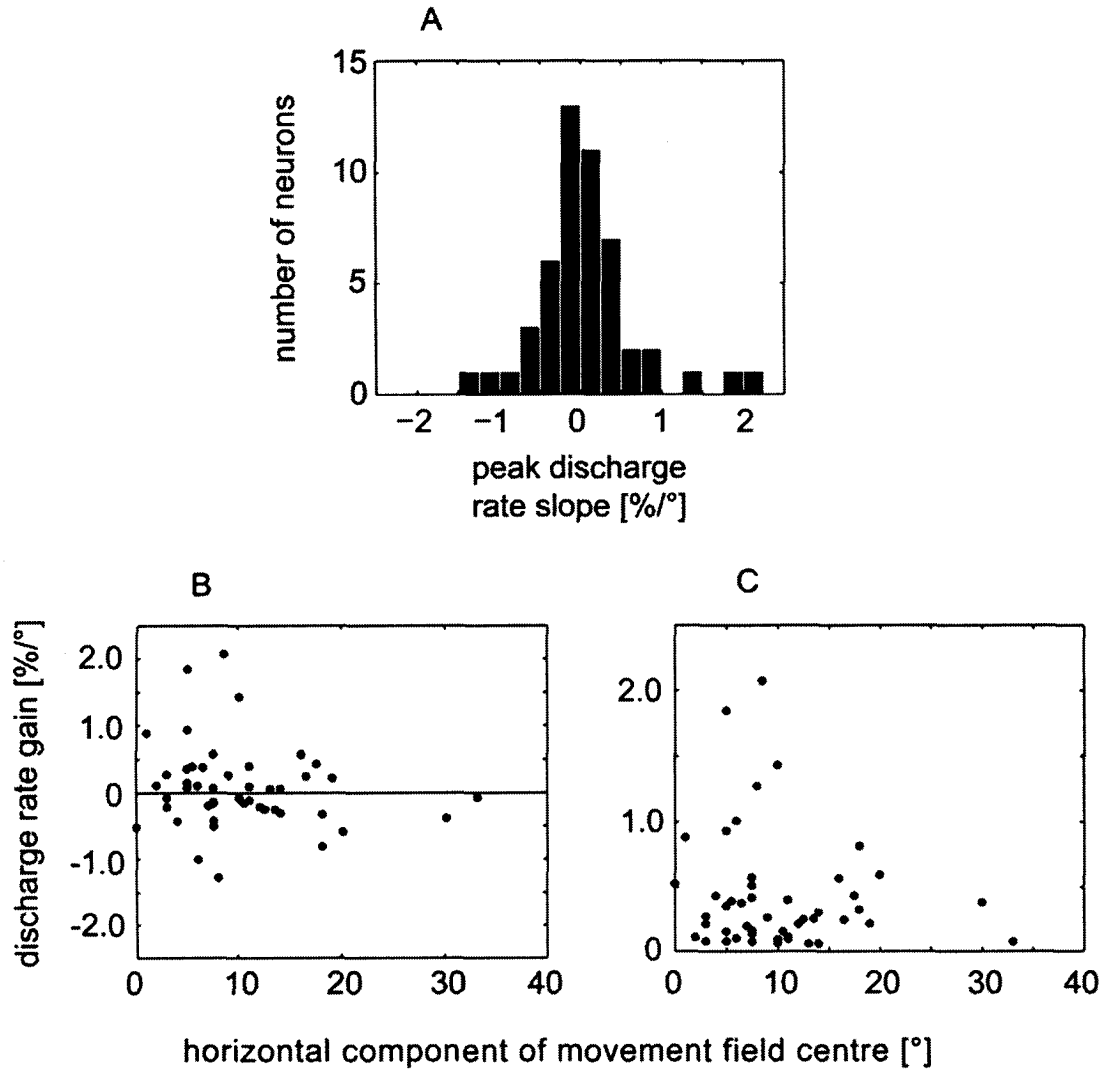

Figure 10. Gain field slopes of all significant linear trends, from the motor period. A: Histogram of gain field slopes, in terms of percentage-change per degree of body-under head rotation. Slopes are evenly distributed between positive and negative values and show no statistical bias for sign. B: Gain field slopes, also in percentage-change per degree of body-under-head rotation, as a function of the horizontal component of movement field centre. No observable trend was found in the distribution of slopes as a function of field centre location. C: Slopes are plotted as magnitudes, as a function of field centre. No observable trend was found in the distribution of slope magnitudes as a function of the movement field centre.

collinearity of the slopes – in other words, there was no preference for either increasing or decreasing peak discharge rates as the body was rotated towards the side of the movement field.

I also examined whether there might be any correlation between the magnitude of the linear trends and the magnitude of the preferred vector. Figure 10, subfigure B, plots the change in peak discharge rate against the horizontal component of the preferred vector for each neuron. Subfigure C shows identical data points, but discards the sign of the trends (thus all trend magnitudes are positive). Weighted linear regressions (using the inverse of the variance as the weighting parameter) on subfigures B and C do not yield statistically significant trends ($P = 0.091$ and $P = 0.18$, respectively). This result strongly suggests no relationship between the magnitude of changes in peak discharge rate across body-under-head positions and the magnitude of the horizontal component of a neuron's preferred vector.

This analysis of peak discharge rate was repeated for the visual and the delay period as well. These results are summarized in Table 2, and can be seen as similar to those for the motor period. The average slope of peak discharge rates for the visual period is similar to the motor period at 0.552 %/°, however, r^2-values are significantly lower. While the linear trends are similar in magnitude between the two periods, less of the variance during the visual period can be accounted for by the trends. A possible explanation for this could be the fact that the typical visual bursts seen in predominantly motor-related neurons are much weaker than the motor bursts. Noise that manifests itself as random changes in spike rate, even as small as 2-3 extra spikes

in the analysis window, has a more pronounced effect during the visual period than the motor period due to the fact that some of the visual bursts peaked at under 100 spikes per second.

	visual	delay	motor
neurons with observed activity	26	28	60
significant ANOVA	26	26	56
significant LTA & linear regression	21	19	50
average slope magnitude [spikes/s/°]	0.850	0.347	0.893
[%/°]	0.552	1.25	0.476
average change over 50° [spikes/s]	42.5	17.4	44.6
[%]	27.6	62.5	23.7
trends with r^2-values > 10%	5	7	33
trends with r^2-values > 20%	2	1	27
trends with r^2-values > 30%	1	1	20
trends with r^2-values > 40%	0	0	14
significant t-test & chi-square test for sign	no	no	no
correlation between slope & field centre	no	no	no

Table 2. Population results for peak discharge rates.

The results for delay period activity are slightly different than for the other periods and much of this stems from the fact that delay activity is not of a burst nature, but of a more uniform and even nature across the analysis window. The average magnitude of the fitted trends is lower at 0.347 spikes/s/°, reflecting the relatively lower discharge rate during the delay period than during the visual and motor bursts. Observed delay activity appeared to have noise similar in magnitude to

the visual period, and as a consequence, r^2-values are also lower than those for the motor burst.

Neurons with visual or delay activity had slopes for those periods that correlated with the respective slope of the motor period (both $P < 0.01$). As such, they were also evenly distributed between positive and negative values, and single-sample t-tests failed to show any statistical evidence for collinearity for either period.

3.4 Population Results - Movement Field Centre and Shape

An analysis on the remaining parameters was performed, identical to that run on peak discharge rates. 5 neurons with incomplete movement fields were excluded from this analysis, and an additional 6 neurons with open movement fields had only a partial analysis performed on them.

Only 4 of 55 neurons had significant linear regressions for changes in movement field centre as a function of body-under-head position. The average change in degrees over 50° of rotation for these 4 neurons was found to be less than 1°. Thus, as with the example neuron, the population of neurons maintained their oculocentric tuning and showed no sign of exhibiting body-centric movement fields.

The general shape of the movement field, as defined by the symmetry and width parameters, did show some statistically significant changes across body-under-head position. 17 neurons showed changes in either one or both of these parameters. 15 of these neurons also had significant changes in peak discharge rate. The most prevalent relationship between these three parameters was that of decreasing width

(11 of 13) and a tendency towards symmetry (7 of 9), for increasing peak discharge rates. Figure 11 illustrates three Gaussian curves with increasing peak discharge rate, with subfigure A showing a constant width, subfigure B showing an increasing width, and subfigure C showing a decreasing width. As can be seen in subfigure C, which best represents the majority of the 17 neurons, decreasing width accompanying an increasing peak tends to focus changes in discharge rate onto saccadic vectors made into the centre of the movement field. This might suggest that body-under-head position effects may be stronger for saccades to the preferred vector than for those to more peripheral locations. A by-product of this phenomenon in asymmetric curves was a tendency towards symmetry, as curves that became mathematically taller also became mathematically more symmetric. This did not mean that the left and right sides of the movement field changed in any significant way, as this was a purely mathematical consequence of raising the peak of the curves.

No other changes in the movement field were observed, and no movement fields were observed to transform from closed to open, or vice versa.

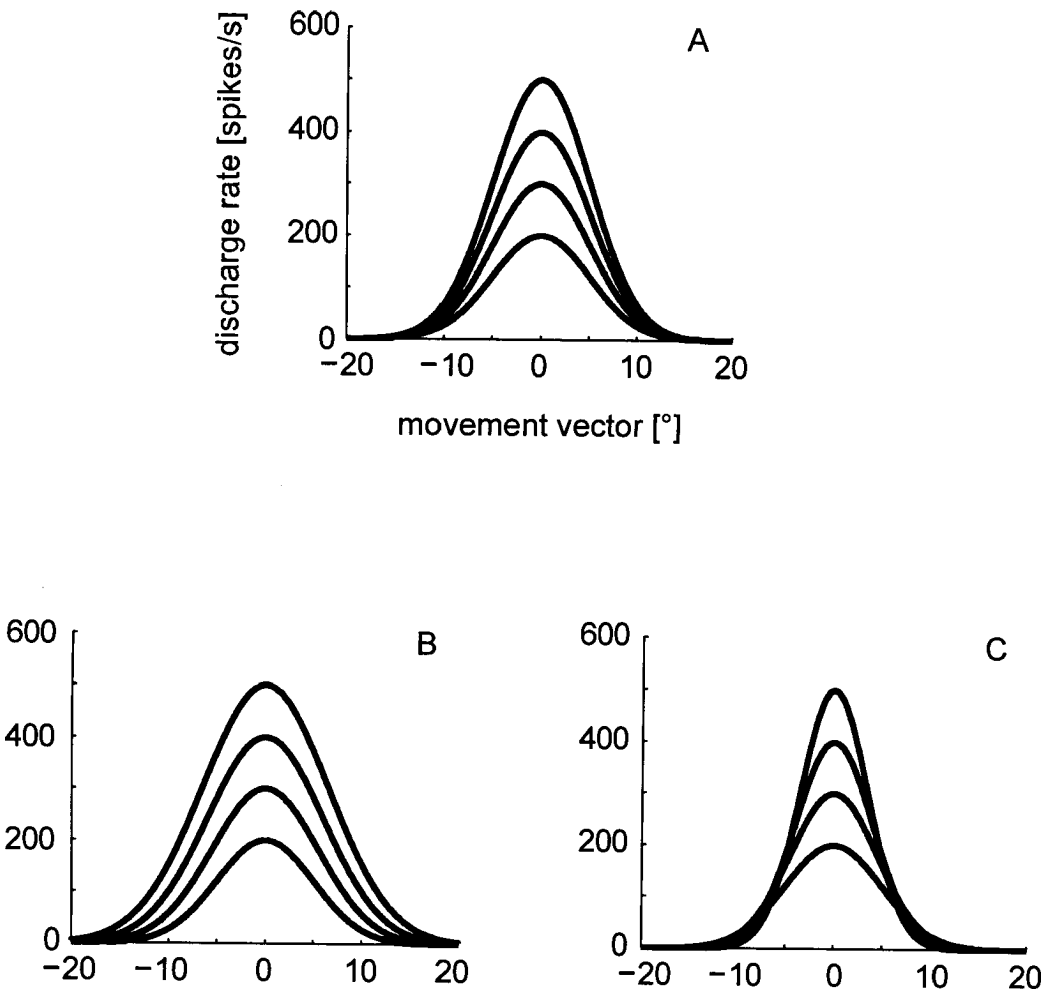

Figure 11. Variations in Gaussian widths and peaks. A: Variations in peak values while maintaining constant width. B: Increasing widths for increasing peaks. C: Decreasing widths for increasing peaks, focusing the increase on values located centrally.

Chapter 4 - Discussion

4.1 General Summary

This present study is the first to examine representations of head-on-body position in the primate superior colliculus. Specifically, I set out to examine the existence of head-position gain fields in the SC, and to characterise their activity compared to previous studies of gain fields in the oculomotor system.

I demonstrated that the movement fields exhibited by SC neurons showed oculocentric tuning for desired gaze displacement, irrespective of the position of the head on the body, but also showed a gain-fielded scaling of amplitudes by head-on-body position. These gain fields were not collinear, but equally likely to rise as to fall as the body was rotated towards the side of the movement field. I will first address the significance of these results in the context of recent studies of gain fields in the oculomotor system, and then I shall consider possible functional roles for the existence of head position gain fields in the SC.

4.2 Comparisons to Previous Studies

Eye position studies in LIP have shown gain modulation in 60% of recorded cells, and the magnitude of this observed effect was 50-78% over 50° of variation in initial position. Discharge rates in LIP are lower than those in the SC, but slopes were similar to those observed in this study, approximately ranging through 0.25 to 3.0 spikes/s/° (Andersen et al., 1990). Head position modulation in LIP has been shown to affect approximately 35% of cells, with changes in discharge rate ranging from 0.25

to 4.0 % per degree of head rotation (Snyder et al., 1998) or the equivalent of 12.5% to 200% over 50° of head rotation. Eye position studies in FEF have shown gain modulation in approximately 50% of neurons with a mean slope of 6.6 %/°. (Cassanello and Ferrera, 2007a). The number of neurons that exhibited gain modulation in this study, and the magnitude of that modulation, is similar to those in other oculomotor brain areas.

Van Opstal and colleagues have shown that eye-in-head position in the SC modulates activity during the motor period in approximately 50% of recorded neurons (Van Opstal et al., 1995). Variations in peak discharge rate during the motor period of their paradigms averaged approximately 1.1%/°, or 3 spikes/s/°. Thus head-on-body position modulation in the SC is very similar in magnitude to eye-in-head modulation found previously, though the results found in this study do show magnitudes slightly lower than those for eye position. One possible explanation for this observation is the fact that experiments involving changes in initial eye position were done in 2-dimensions (with initial eye position variable along both the horizontal and vertical axis), while the experimental setup in this study restricted body-under-head position to locations along the horizontal axis. I was unable to vary the position of the head relative to the body along the vertical axis, and thus only horizontal gain modulation effects could be induced and observed. Many of the neurons in my study had preferred vectors with significant vertical components, thus it is possible that they also had gain fields that were most sensitive to oblique changes

in head position, with respect to the torso. My analysis of these neurons extracted only the horizontal component of their gain field sensitivities.

A second observation of this study is that gain modulation had no detectable collinearity: gain field slopes were equally distributed towards and away from the side of the movement field. Eye position gain fields in the SC were found to slope in all directions, but had a partial collinearity with 50% of slopes aligning in the general direction of the movement field (±45°), with the remainder of the slopes orthogonal or in the opposite direction to the movement field (Van Opstal et al., 1995). In the FEF, eye position gain fields were found to be strongly aligned, but in the opposite direction of the movement field (approximately 80% being anti-collinear) (Cassanello and Ferrera, 2007a). Head position signals in LIP were found to have strongly parallel gain fields as well, with the vast majority of the gain field neurons exhibiting collinearity (Brotchie et al., 1995). Functional roles for populations of neurons with directional gain fields have been suggested by computational models, such as visual remapping by vector subtraction (Cassanello and Ferrera, 2007b) and coordinate transformation (Andersen and Buneo, 2002; Andersen and Buneo, 2003). Noncollinear populations, however, such as those found in this study, have also been shown to function effectively in models that output vectors in multiple frames of reference (Van Opstal and Hepp, 1995b). Thus the head position gain fields that are described in this present study may help with the decoding of the gaze displacement command in various frames.

4.3 Possible Functional Roles For Gain Fields in the SC

Could gain fields in the SC play a role in a coordinate transformation from oculocentric to craniocentric or body-centric reference frames, and if so, what would be the purpose of such a coordinate transformation? The representation of gaze commands as movement vectors can be considered a relatively high-level method of encoding, and such a representation may have little to do with the actual patterns of eye and neck muscle activation required to execute the movement (consider the example illustrated in Figure 1, subfigure B). Coordinating neck muscle activation is complex and depends strongly on initial and final head position, even for head movements with similar kinematics (Corneil et al., 2001). Transforming a movement into craniocentric and body-centric coordinates may be one of the many steps required to ultimately transform the movement into individual muscle-centric coordinates as needed for the motor neurons that execute the gaze shift. Initial positional information is critical for this process, but where this transformation actually occurs is uncertain.

As this study shows that initial head position influences SC activity, it is possible that the SC is involved in a network that performs this transformation. Van Opstal and colleagues suggested that two-dimensional craniocentric eye position may be extracted from a network that includes weighted projections of gain field neurons in the SC (Van Opstal et al., 1995). Thus, the same SC neurons may effectively transmit the gaze command in both reference frames (oculocentric and craniocentric). Accompanying their study, they also performed computational

simulations to determine the feasibility of their model (Van Opstal and Hepp, 1995). Their results indicated that a model with gain fields that had slopes distributed randomly in two dimensions was indeed able to produce positional information through weighted projections.

While this present study only examined head position effects along one dimension, and showed an equal likelihood of collinear and noncollinear gain fields, if the existence of neurons with orthogonal gain fields is also assumed (that is, gain fields sensitive to vertical changes in head position), then the model of Van Opstal and colleagues may be extended to include initial head position. This extension could have the SC outputting the gaze displacement command in oculocentric coordinates, with sufficient information in this signal (through gain modulation) to allow the extraction of eye position in eye-in-head coordinates, and head position in head-on-body coordinates. With this information present, and with appropriate downstream circuitry, it is theoretically possible to extract the gaze command in both craniocentric and body-centric coordinates. Whether eye and head position gain fields exist in the same cell, and if so, how eye *and* head position can be extracted from these cells, are currently open questions. While computational studies suggest that gain fields modulated by multiple inputs can provide spatial output in multiple frames, the complexity in such systems increases exponentially as additional dimensions are added (Andersen and Buneo, 2002; Andersen and Buneo, 2003).

Alternatively, one could also consider the possibility that eye and head position gain fields are not as independent as one might think. No study has

simultaneously examined both eye and head position gain fields in the SC to test for any interaction. Campos and colleagues, and Van Opstal and colleagues, examined gain fields while only varying eye-in-head position (Campos et al., 2006; Van Opstal et al., 1995). As both the head and torso were fixed in space, their craniocentric eye position gain fields could also be defined as body-centric eye position gain fields. In other words, the modulating factor may not exclusively be the position of the eye relative to the head, but the eye relative to the body. This modulation could be detected by varying initial eye position, with the body and head fixed in space, but it could also be detected by varying body-under-head position, as this present study did. Whether the population of neurons revealed in this study are the same as those with eye position gain fields remains to be examined. Experiments would have to be performed that could discriminate between eye and head position gain fields, and could also determine whether neurons have gaze (relative to the body) position gain fields. This would involve both independent and concurrent variations of eye-in-head and head-on-body position.

4.4 Possible Sources of Head Position Information

In this study I rotated the body under a stable and immobile head to determine if the position of the head relative to the body affected movement fields in the SC. This rotation stretched neck muscle fibres and presumably generated proprioceptive signals conveying information regarding the degree of rotation (Richmond and Abrahams, 1975; Bakker and Richmond, 1982). Rotating the head

above an immobile body would have also succeeded in generating such proprioceptive signals, and may superficially appear to be an easier experiment to perform. This technique was avoided, however, as it would introduce confounding vestibular inputs which would make it impossible to determine whether gain modulation was occurring as a result of proprioception (representing head-on-body position) or head-in-space rotation.

There are several means through which proprioceptive information regarding head-on-body position could enter into the SC. While it has been shown that LIP sends projections to the SC (Blatt et al., 1990; Paré and Wurtz, 1997), it is unclear whether LIP neurons with head position gain fields specifically do so. But if these projections were to exist, then head position information would have a direct path to the SC. It is possible that the gain fields that I have shown in the SC are a reflection of the gain fields present in LIP, however, this interpretation may be at odds with the fact that gain fields in LIP are mostly collinear (Brotchie et al., 1995) while those that I have found are not.

Head position information may also come to the SC through other paths. Studies in anesthetised cats in which neck muscle nerves were stimulated showed activity elicited in the SC (Abrahams and Rose, 1975). Similarly, neck muscle afferents have been shown to terminate in areas of the brainstem that have been shown to have projections to the primate SC (Edney and Porter, 1986).

It is unknown whether single or multiple sources are responsible for the effects described in this study. A possible experiment to determine which paths may

be involved would have LIP deactivated – if head position gain fields disappear from the SC, this would support the supposition that LIP is the path through which this information is conveyed. Alternatively, gain fields in the SC may remain identical, or may be modified in some way, suggesting alternate sources or combinations of sources for positional information. Deactivation of brainstem areas that may relay positional information could prove cumbersome, as these areas are more difficult to localize and isolate, and may result in unintended gaze-related consequences.

While the mere existence of head position representations in the SC suggest a functional role, one must acknowledge the possibility that it may simply reflect the SC's position in the oculomotor system, downstream of LIP. Projections from LIP that carry head position gain fields may be influencing the SC such that gain modulation is also present as a residual effect. Unless a system exists downstream of the SC that extracts positional information, the population of noncollinear gain fields may cancel out, with the result that the only meaningful information to leave the SC would be a gaze displacement command in oculocentric coordinates. This would place the SC outside of the network that performs the transformation of this command into eye-in-head and head-on-body coordinates.

4.4 General Conclusions

The results of this study show that proprioceptive representations of head-on-body position gain modulate activity in the primate superior colliculus. Eye and head position gain fields have been found in the oculomotor system in previous studies,

but this is the first to describe head position gain fields in the SC. The one-dimensional gain fields described in this thesis approach the strength of the two-dimensional eye position gain fields found in previous experiments. Gain fields in the oculomotor system have been found to align themselves with the preferred gaze vector to varying degrees, and though a complete characterisation of gain fields was not possible in this study (as head position was only varied along one dimension), gain field alignment appeared equally distributed along positive and negative horizontal directions, showing no evidence of collinearity.

The role of gain fields in the SC may be similar to those suggested for gain fields in other brain areas: to participate in some form of coordinate transformation. The gaze displacement command must eventually be converted into activation patterns specific to the muscles involved, and this conversion must involve transformations of the oculocentric command output from the SC. Theoretical studies suggest that modulation of this command by initial head position could be one step in this process. Neural activity in the SC, in addition to encoding the gaze vector, may contain sufficient information to allow for the extraction of initial and final position in multiple reference frames by downstream oculomotor centres.

References

Abrahams VC, Rose PK (1975) Projections of extraocular, neck muscle, and retinal afferents to superior colliculus in the cat: their connections to cells of origin of tectospinal tract. J Neurophysiol 38:10-18.

Andersen RA, Bracewell RM, Barash S, Gnadt JW, Fogassi L (1990) Eye position effects on visual, memory, and saccade-related activity in areas LIP and 7a of macaque. J Neurosci 10:1176-1196.

Andersen RA, Buneo CA (2002) Intentional maps in posterior parietal cortex. Annu Rev Neurosci 25:189-220.

Andersen RA, Buneo CA (2003) Sensorimotor integration in posterior parietal cortex. Adv Neurol 93:159-177.

Bakker DA, Richmond FJ (1982) Muscle spindle complexes in muscles around upper cervical vertebrae in the cat. J Neurophysiol 48:62-74.

Blatt GJ, Andersen RA, Stoner GR (1990) Visual receptive field organization and cortico-cortical connections of the lateral intraparietal area (area LIP) in the macaque. J Comp Neurol 299:421-445.

Brotchie PR, Andersen RA, Snyder LH, Goodman SJ (1995) Head position signals used by parietal neurons to encode locations of visual stimuli. Nature 375:232-235.

Bruce CJ, Goldberg ME (1985) Primate frontal eye fields. I. Single neurons discharging before saccades. J Neurophysiol 53:603-635.

Buschman TJ, Miller EK (2007) Top-down versus bottom-up control of attention in the prefrontal and posterior parietal cortices. Science 315:1860-1862.

Campos M, Cherian A, Segraves MA (2006) Effects of eye position upon activity of neurons in macaque superior colliculus. J Neurophysiol 95:505-526.

Cassanello CR, Ferrera VP (2007a) Computing vector differences using a gain field-like mechanism in monkey frontal eye field. J Physiol 582:647-664.

Cassanello CR, Ferrera VP (2007b) Visual remapping by vector subtraction: analysis of multiplicative gain field models. Neural Comput 19:2353-2386.

Corneil BD, Olivier E, Richmond FJ, Loeb GE, Munoz DP (2001) Neck muscles in the rhesus monkey. II. Electromyographic patterns of activation underlying postures and movements. J Neurophysiol 86:1729-1749.

Duhamel JR, Colby CL, Goldberg ME (1992) The updating of the representation of visual space in parietal cortex by intended eye movements. Science 255:90-92.

Edelman JA, Goldberg ME (2001) Dependence of saccade-related activity in the primate superior colliculus on visual target presence. J Neurophysiol 86:676-691.

Edney DP, Porter JD (1986) Neck muscle afferent projections to the brainstem of the monkey: implications for the neural control of gaze. J Comp Neurol 250:389-398.

Elsley JK, Nagy B, Cushing SL, Corneil BD (2007) Widespread presaccadic recruitment of neck muscles by stimulation of the primate frontal eye fields. J Neurophysiol 98:1333-1354.

Everling S, Munoz DP (2000) Neuronal correlates for preparatory set associated with pro-saccades and anti-saccades in the primate frontal eye field. J Neurosci 20:387-400.

Freedman EG, Sparks DL (1997a) Eye-head coordination during head-unrestrained gaze shifts in rhesus monkeys. J Neurophysiol 77:2328-2348.

Freedman EG, Sparks DL (1997b) Activity of cells in the deeper layers of the superior colliculus of the rhesus monkey: evidence for a gaze displacement command. J Neurophysiol 78:1669-1690.

Freedman EG, Stanford TR, Sparks DL (1996) Combined eye-head gaze shifts produced by electrical stimulation of the superior colliculus in rhesus monkeys. J Neurophysiol 76:927-952.

Fuchs AF, Robinson DA (1966) A method for measuring horizontal and vertical eye movement chronically in the monkey. J Appl Physiol 21:1068-1070.

Gandevia SC, McCloskey DI, Burke D (1992) Kinaesthetic signals and muscle contraction. Trends Neurosci 15:62-65.

Isa T, Sasaki S (2002) Brainstem control of head movements during orienting; organization of the premotor circuits. Prog Neurobiol 66:205-241.

Judge SJ, Richmond BJ, Chu FC (1980) Implantation of magnetic search coils for measurement of eye position: an improved method. Vision Res 20:535-538.

Keppel G, Wickens TD (2004) Design and Analysis: A Researcher's Handbook. Prentice Hall.

Leigh RJ, Zee DS (2006) The Neurology of Eye Movements. New York: Oxford University Press, Inc.

Matthews PB (1982) Where does Sherrington's "muscular sense" originate? Muscles, joints, corollary discharges? Annu Rev Neurosci 5:189-218.

McCluskey MK, Cullen KE (2007) Eye, head, and body coordination during large gaze shifts in rhesus monkeys: movement kinematics and the influence of posture. J Neurophysiol 97:2976-2991.

Miyashita N, Hikosaka O (1996) Minimal synaptic delay in the saccadic output pathway of the superior colliculus studied in awake monkey. Exp Brain Res 112:187-196.

Moschovakis AK, Scudder CA, Highstein SM (1996) The microscopic anatomy and physiology of the mammalian saccadic system. Prog Neurobiol 50:133-254.

Munoz DP, Wurtz RH (1995) Saccade-related activity in monkey superior colliculus. I. Characteristics of burst and buildup cells. J Neurophysiol 73:2313-2333.

Paré M, Wurtz RH (1997) Monkey posterior parietal cortex neurons antidromically activated from superior colliculus. J Neurophysiol 78:3493-3497.

Pouget A, Snyder LH (2000) Computational approaches to sensorimotor transformations. Nat Neurosci 3 Suppl:1192-1198.

Richmond FJ, Abrahams VC (1975) Morphology and distribution of muscle spindles in dorsal muscles of the cat neck. J Neurophysiol 38:1322-1339.

Robinson DA (1964) The mechanics of human saccadic eye movement. J Physiol 174:245-264.

Robinson DA (1972) Eye movements evoked by collicular stimulation in the alert monkey. Vision Res 12:1795-1808.

Salinas E, Thier P (2000) Gain modulation: a major computational principle of the central nervous system. Neuron 27:15-21.

Scudder CA, Moschovakis AK, Karabelas AB, Highstein SM (1996a) Anatomy and physiology of saccadic long-lead burst neurons recorded in the alert squirrel monkey. I. Descending projections from the mesencephalon. J Neurophysiol 76:332-352.

Scudder CA, Moschovakis AK, Karabelas AB, Highstein SM (1996b) Anatomy and physiology of saccadic long-lead burst neurons recorded in the alert squirrel monkey. II. Pontine neurons. J Neurophysiol 76:353-370.

Segraves MA, Goldberg ME (1987) Functional properties of corticotectal neurons in the monkey's frontal eye field. J Neurophysiol 58:1387-1419.

Snyder LH, Grieve KL, Brotchie P, Andersen RA (1998) Separate body- and world-referenced representations of visual space in parietal cortex. Nature 394:887-891.

Sommer MA, Wurtz RH (2002) A pathway in primate brain for internal monitoring of movements. Science 296:1480-1482.

Sommer MA, Wurtz RH (2000) Composition and topographic organization of signals sent from the frontal eye field to the superior colliculus. J Neurophysiol 83:1979-2001.

Sparks D, Rohrer WH, Zhang Y (2000) The role of the superior colliculus in saccade initiation: a study of express saccades and the gap effect. Vision Res 40:2763-2777.

Sparks DL (2002) The brainstem control of saccadic eye movements. Nat Rev Neurosci 3:952-964.

Sparks DL, Hartwich-Young R (1989) The deep layers of the superior colliculus. Rev Oculomot Res 3:213-255.

Sparks DL, Holland R, Guthrie BL (1976) Size and distribution of movement fields in the monkey superior colliculus. Brain Res 113:21-34.

Stanton GB, Goldberg ME, Bruce CJ (1988) Frontal eye field efferents in the macaque monkey: II. Topography of terminal fields in midbrain and pons. J Comp Neurol 271:493-506.

Thompson KG, Hanes DP, Bichot NP, Schall JD (1996) Perceptual and motor processing stages identified in the activity of macaque frontal eye field neurons during visual search. J Neurophysiol 76:4040-4055.

Tigges J, Tigges M (1981) Distribution of retinofugal and corticofugal axon terminals in the superior colliculus of squirrel monkey. Invest Ophthalmol Vis Sci 20:149-158.

Van Opstal AJ, Hepp K (1995) A novel interpretation for the collicular role in saccade generation. Biol Cybern 73:431-445.

Van Opstal AJ, Hepp K, Suzuki Y, Henn V (1995) Influence of eye position on activity in monkey superior colliculus. J Neurophysiol 74:1593-1610.

Wang X, Zhang M, Cohen IS, Goldberg ME (2007) The proprioceptive representation of eye position in monkey primary somatosensory cortex. Nat Neurosci 10:640-646.

Wurtz RH, Sommer MA, Paré M, Ferraina S (2001) Signal transformations from cerebral cortex to superior colliculus for the generation of saccades. Vision Res 41:3399-3412.

Xing J, Andersen RA (2000) Models of the posterior parietal cortex which perform multimodal integration and represent space in several coordinate frames. J Cogn Neurosci 12:601-614.

Appendix 1 - Ethics Approval

October 17, 2004

"This is the 1st Renewal of this protocol"
"A Full Protocol submission will be required in 2007"

Dear Dr. Cornell:

Your "Application to Use Animals for Research or Teaching" entitled:

"Sensory and motor roles for neck muscles in visually-guided actions: Neural mechanisms underlying recruitment and kinesthesia"
Funding Agency-- CIHR Grant # MOP 64202

has been approved by the University Council on Animal Care. This approval is valid from December 1, 2004 to November 30, 2005. The number for this project remains as #2003-104-11.

1. This number must be indicated when ordering animals for this project.
2. Animals for other projects may not be ordered under this number.
3. If no number appears please contact this office when grant approval is received.
   If the application for funding is not successful and you wish to proceed with the project, request that an internal scientific peer review be performed by the Animal Use Subcommittee office.
4. Purchases of animals other than through this system must be cleared through the ACVS office. Health certificates will be required.

ANIMALS APPROVED				FOR 1 YR.	PAIN LEVEL -D
Primates	-	Rhesus 3-8 yrs./4-12 kg	M -	2	

STANDARD OPERATING PROCEDURES
Procedures in this protocol should be carried out according to the following SOPs. Please contact the Animal Use Subcommittee office (661-2111 ext. 86770) in case of difficulties or if you require copies.
SOP's are also available at http://www.uwo.ca/animal/acvs
310 Holding Period Post Admission
320 Euthanasia
321 Early Euthanasia/Rodents

REQUIREMENTS/COMMENTS
Please ensure that individual(s) performing procedures on live animals, as described in this protocol, are familiar with the contents of this document.

CHANGES New staff added

c.c. Approved Protocol - B. Cornell, T. Admans, W. Lagerwerf
Approval Letter - T. Admans, W. Lagerwerf